Ulm University Hospital

Department of Neurology

Director: Prof. Dr.med. Albert Christian Ludolph

Synaptic Circular RNAs: a new class of regulators of acute response and repair in TBI

Dissertation

Submitted to the

Medical Faculty of University of Ulm

For the Doctoral Degree of Medicine (Dr. med.)

Presented by

Zhenghui Li

Born in Kaifeng city, Henan Province, P. R. China

2021

Dean of the Faculty of Medicine: Prof. Dr. rer. nat. Thomas Wirth

1st reviewer: Prof. Dr. Francesco Roselli

2nd reviewer: Prof. Dr. Bernd Knöll

Date of defense: 02.06.2022

Parts of this work have already been published elsewhere:

Florian Olde Heuvel, Sarah Holl, Akila Chandrasekar, **Zhenghui Li**, Yibin Wang, Rida Rehman, Philip Förstner, Daniela Sinske, Annette Palmer, Diana Wiesner, Albert Ludolph, Markus Huber-Lang, Borna Relja, Thomas Wirth, Tamás Röszer, Bernd Baumann, Tobias Boeckers, Bernd Knöll, Francesco Roselli. *STAT6 mediates the effect of ethanol on neuroinflammatory response in TBI. Brain, behavior, and immunity, 2019. 81: p. 228-246.*

Conference:

Poster of *Synaptic Circular RNAs: a new class of regulators of acute response and repair in TBI* in International Neurotrauma Symposium 2020; **Zhenghui Li,** Florian olde Heuvel, Francesco Roselli

List of Content

List of Content ..... **I**
Abbreviations ..... **III**
1 Introduction **1**
1.1 General introduction of traumatic brain injury 1
1.1.1 The role of excitotoxicity transmitter and excitotoxicity in TBI 2
1.1.2 The role of calcium overload in TBI 3
1.1.3 The role of release of reactive oxygen species in TBI 3
1.1.4 The role of neuroinflammation in TBI 4
1.1.5 The role of apoptosis in TBI 5
1.1.6 The clinical features and biological markers of TBI 6
1.2 The general introduction and functions of circRNA 7
1.2.1 The general introduction of circRNAs in central nervous syatem 9
1.2.2 The role of circRNAs in Neurological Diseases 10
1.2.3 CircRNAs as neurological diseases biomarker 11
1.3 The aim of this study 12
2 Materials and methods **14**
2.1 Materials 14
2.1.1 Laboratory equipment 14
2.1.2 Plastic materials 15
2.1.3 Equipment for hippocampus injection 16
2.1.4 Chemicals and drugs 17
2.1.5 Antibodies for co-staining with BaseScope 18
2.2 Methods 19
2.2.1 Animal model and husbandry 19
2.2.2 Human brain sample collection 19
2.2.3 RNA isolation and qRT-PCR 21
2.2.4 Cell culture and transfection 25
2.2.5 Recombinant adeno-associated viruses produceAAV(rAVV) vectors 26
2.2.6 Hippocampus injection and TBI operation 26
2.2.7 Behaviour experiment 28
2.2.8 Mouse perfusion and brain dissection and fixation 29

2.2.9 Cryostat sections preparation 31
2.2.10 BaseScope and co-immunofluorescence staining 31
2.2.11 Image acquisition and analysis 34
2.2.12 Statistics 34

3 Results 36
3.1 The spatio-temporal expression of cirular RNAs in mouse brain 36
3.2 CircRNAs profiling in TBI mouse hippocampus tissues after TBI 37
3.3 The expression of circKlhl2 and circGrin2a in TBI 40
3.4 The basic information of circKlhl2 42
3.5 The expression level of circKlhl2 in different regions of hippocampus 45
3.6 Generation of circKlhl2 interference and overexpression plasmids 48
3.7 CircKlhl2 may regulate BDNF via miR-30a/d-5p and miR-34a-5p 49
3.8 Overexpression of circKlhl2 may ameliorate Anxiety-Like behavior 51
3.9 Overexpression of circKlhl2 enhanced spatial memory 52
3.10 Overexpression of circKlhl2 may Enhance short-term learning memory 53
4 Discussion 55
5 Summary 59
6 Reference 61
7 Acknowledgements 72
8 Curriculum vitae 73

Abbreviations

3R	Replacement, reduction,refinement
°C	Degree Celsius

A

AAV	Adeno-associated virus
AMPA	α-amino-3-hydroxy-5-methyl-4-isoxazolepropionic acid
ABCB10	ATP-binding cassette sub-family B member 10
AKT3	AKT serine/threonine kinase 3
ALS	Amyotrophic Lateral Sclerosis
AIS	Acute Ischemic Stroke
AD	Alzheimer disease
APP	Amyloid Beta Precursor Protein
ALS2	Alsin Rho Guanine Nucleotide Exchange Factor ALS2
AKAP	A-Kinase Anchoring Protein
ANOVA	Analysis of variance
Amp	Ampicillin
AMP	Amplify

B

BBB	Blood-Brain Barrier
BSA	Bovine Serum Albumin
Bcl-2	B-cell lymphoma 2
BH3	Bcl-2 homology

BDNF	Brain-derived neurotrophic factor

C

CT	Computed Tomography
CSF	cerebral spinal fluid
Ca^{2+}	Calcium
ciRNA	Circular intronic RNA
cDNA	complementary DNA
CT value	Cycle threshold value
CNS	Central Nervous System
Con	Control
CSF	Cerebrospinal fluid
ceRNA	Competing endogenous RNA

D

DNA	Deoxyribonucleic acid
Dlgap	Disks large-associated protein
dNTPs	Deoxynucleotides
Dlg	Discs Large MAGUK Scaffold Protein
DMEM	Dulbecco's Modified Eagle Medium
DG	Dentate gyrus
DAPI	4′,6-diamidino-2-phenylindole

E

EAAT2	Excitatory amino acid transporter-2
ERS	Endoplasmic reticulum stress

EIciRNA	Exon-intron circular RNAs

H

HMG20A	High mobility group protein 20A
HCl	Hydrochloric acid
HECTD1	HECT domain E3 ubiquitin protein ligase 1
Homer	Homer protein homolog 1

I

Iba-1	Ionized calcium-binding adapter molecule-1
ICAM-1	Intercellular adhesion molecule 1
IFN-γ	Interferon gamma
IL	Interleukin
ICU	Intensive Care Unit
i.p.	Intraperitoneal(ly)
Ipsi	Ipsilateral
IRES	Internal ribosome entry site

K

Klhl2	Kelch Like Family Member 2
KD	Knock down
Kcnn2	Potassium Calcium-Activated Channel Subfamily N Member 2

L

l	Litre

LSM	Laser scanning microscope

M

miRNA	microRNA
RBPs	RNA binding proteins
mg	Milligram
mRNA	messenger RNA
Myo5a	Myosin-Va
min	Minutes
ml	Millilitre
mm	Millimeter
MN	Motor neuron
MAP2	Microtubule-associated protein 2
msec	Millisecond

N

NMDA	N-methyl-D-aspartic acid receptor
MAPK	Mitogen-activated protein kinase
NaCl	Sodium chloride
Nlgn1	Neuroligin-1
Ncam	Neural cell adhesion molecule
Nm	Nanomolar
nm	Nanometre
N2a cells	Neuro2a cells
NC	Negative control

NLR	Novel location recognition
NOR	Novel object recognition

O

OFR	Oxygen free radicals
O2	Oxygen
OE	Overexpression
Nlgn1	Neuroligin-1
OFT	Open field test

P

PBS	Phosphate buffered saline
PFA	Paraformaldehyde
PSD-95	Postsynaptic density protein 95
PTK	Protein tyrosine kinases
PAIP2	Polyadenylate-binding protein-interacting protein 2
PEI	Polyethylenimine

Q

Qrt-PCR	Real-Time Quantitative Reverse Transcription PCR

R

ROS	Reactive oxygen species
Raav	Recombinant adeno-associated virus
RNA	Ribonucleotide Acid

RT	Room temperature
RTK	Receptor tyrosine kinases
RNAse R	Ribonuclease R
RT buffer	Reverse transcription buffer
R	Reverse
Rims1	Regulating Synaptic Membrane Exocytosis 1
Rps6kc1	Ribosomal Protein S6 Kinase C1

S

S	Sham
Stx6	Syntaxin-6
Slc8a1	Solute Carrier Family 8 Member A1
Strn3	Striatin 3
SAP	Spontaneous alternation performance

U

UV	Ultraviolet
µl	Microlitre
µm	Micrometre
USA	United States of America

V

VEGF-A	Vascular Endothelial Growth Factor-A
VAChT	Vesicular acetylcholine transporter

W

WT	Wild type

1 Introduction

1.1 General introduction of traumatic brain injury

Traumatic brain injury (TBI), also known as an intracranial injury, is an injury to the brain caused by an external force, which includes falls, vehicle accidents and physical violence. Brain trauma occurs as a consequence of a sudden acceleration or deceleration within the cranium or by a complex combination of both movement and sudden impact. In recent years, with the widespread use of transportation, the incidence of traumatic craniocerebral injury has gradually increased. TBI results in a high risk of neurological dysfunction or, more seriously, deprives patients of their self-sufficiency, which places an enormous burden on society and families. Despite its high incidence and morbidity, there are very limited treatment options for improving outcome after traumatic brain injury (TBI)[1, 72].

TBI pathogenesis is a complex process that results from primary and secondary injuries that lead to temporary or permanent neurological deficits. The primary deficit is related directly to the primary external impact to the brain. The secondary injury occurs minutes to days after the primary impact and consists of a molecular, chemical, and inflammatory cascade responsible for subsequent cerebral damage [83]. Additionally, secondary brain damage after TBI represents a multifaceted danger that adversely affects the disease course resulting in persistent neurological impairments. The biochemical, cellular, and physiological events that occur during the primary injury usually develop into delayed and prolonged secondary injuries, lasting from hours to years[47]. More precisely, BBB,(blood-brain-barrier) dysfunction caused by TBI insult allows transmigration of immune cells into the injured brain parenchyma[16]. Activated leukocytes, microglia and astrocytes produce ROS (reactive oxygen species) and inflammatory molecules such as cytokines and chemokines that contribute to demyelination and disruption of axonal cytoskeleton, leading to axonal swelling and accumulation of transport proteins at the terminals, hence compromising neuronal activity[29]. Progressive axonal damage results in neurodegeneration. In addition, the proliferation of astrocytes in the diseased site causes the formation of glial scars, which creates an impermissible environment that hinders axon regeneration[10, 52]. On the other hand, traumatic brain injury can result in excitotoxicity of the central nervous system which causes excessive release of excitatory amino acids, such as glutamate and aspartate from presynaptic nerve terminals. Due to impaired uptake,

the diffusion of glutamate outside the synapse may lead to an increase in the extra-synaptic glutamate signal, activation of cell death pathways and loss of synaptic transmission[27]. The postsynaptic membrane allows calcium ions to flow in. These events, along with the release of ions from the intracellular storage, lead to the production of ROS and activation of calpain. Mitochondrial dysfunction results from the death of caspase-dependent and independent neuronal cells [99, 122, 125].

1.1.1 The role of excitatory neurotransmitters and excitotoxicity in TBI

In mammals, amino acids such as glutamic acid and aspartic acid are considered to be the main excitatory signal transmitters in the brain. Studies in animals and humans have shown that BBB breakdown and cell death of neurons after TBI can cause excessive release of excitatory amino acids, such as glutamate and aspartate from presynaptic nerve terminals, resulting in excitotoxicity of the nervous system post TBI[43]. Glutamate receptors are located on the cell membranes of most neuronal and glial cells, including the families of NMDA (GluN1-1a/b, GluN1-2a/b, GluN1-3a/b and GluN1-4a/b), AMPA (GluR1-4) and kainate receptors (GluR5-9, KA1 and KA2)[9, 93]. Therefore, extracellular glutamate content determines the degree of receptor activation. Massive amounts of extracellular glutamate, which results in an excessive glutamate receptor activation can cause excitotoxicity [39, 67, 97].. Both animal and human studies have confirmed that the glutamate content of the extracellular fluid in the acute phase after brain trauma can increase massively [66].

Several mechanisms are involved in excitotoxicitxy after traumatic brain injury. On the one hand, continuous depolarization can promote a large amount of extracellular Na^+ and Ca^{2+} influx which can directly lead to neuronal edema[86], and the restoration of the Na^+/K^+ gradient consumes energy[22, 126]. On the other hand, the increase of intracellular Ca2+ concentration induces both cell damage, caused by oxidative stress, and also activates various degrading enzymes (such as lipase, protease and endonuclease)[94], damaging lipids[30], functional proteins and cellular DNA, which finally results in apoptosis[13, 109].

In summary, excessive stimulation of glutamate receptors caused by the massive release of excitatory neurotransmitters leads to prolonged post-traumatic oxidative stress and excitotoxic cell death, which correlate with increased mortality rate and worsened neurological outcome.

1.1.2 The role of calcium overload in TBI

Under physiological conditions, Ca^{2+} regulates in the synthesis and release of neurotransmitters, the maintenance of nerve excitability, synaptic plasticity, and the activity of multiple enzymes[109]. It is an important "second messenger" for neuronal information transmission and it is released in the cytoplasm. At the same time, there is a dynamic balance between the recycling of calcium ions, which ensures the stability of the electrolytes in the internal environment of the cell[21]. The concentration of Ca^{2+} in neurons increased significantly after TBI. Deshpande and Sun et al. measured Ca^{2+} in hippocampal neurons of TBI treated rats and found that Ca^{2+} increased significantly on the first and keeps increasing the following days until seventh day after trauma [100]. Learning was impaired until 30 days after injury, shown by the results of the Moris water maze. Once the Ca2+ levels returned to baseline, the cognitive function of the rats also recovered [23, 100]. Intracellular calcium overload may further activate intracellular proteases and phospholipases, destroying the integrity of neuronal and glia cells. In addition, a large amount of calcium influx can decouple the oxidative phosphorylation electron transport chain, and can also activate the caspase apoptosis signaling pathway, leading to cell edema or apoptosis[37, 117].

1.1.3 The role of release of reactive oxygen Species in TBI

Under physiological conditions, the reactive oxygen species (ROS) play a unique physiological role, including killing harmful microorganisms or mutant cells, detoxification of drugs and toxins, and immune regulation. Under pathological conditions, there is imbalance in production and removal (or antagonism) of oxygen free radicals , which causes cellular stress or damage, called oxidative stress[57, 79]. Excessive ROS can cause lipid peroxidation[78], DNA fragment damage, mitochondrial damage[73] through the reaction of polyunsaturated fatty acids on the cell membrane (forming lipoperoxy radicals)(add reference nr 3), and affect the blood-brain barrier, which results in further brain tissue damage[73].. The increase in mitochondrial membrane permeability and the oxidation of membrane proteins lead to changes in ion mobility[85]. For example, abnormal Ca^{2+} accumulation has a profound effect on prolonged excitotoxicity[101]. In short, the sustained release of ROS in TBI and the associated increase in ROS-mediated lipid

peroxidation have an adverse effect on brain plasticity, cerebral blood flow, and promote immunosuppression.

1.1.4 The role of neuroinflammation in TBI

The characteristic neuroinflammatory response to TBI is well described and includes two main parts, a cellular inflammatory response and a transmitter inflammatory response[72, 96]. It is generally believed that neuroinflammation plays a dual role in the pathological process of craniocerebral injury. A moderate inflammatory response has been shown to have protective effects for the body [71]. However, the excessive inflammatory response generates multiple complications after severe trauma; early inflammation is caused by the release of neurotoxic substances which aggravates brain damage. However, the same substance can promote the repair of damaged tissue in later stages, but the full time course of most substances are still not well understood [110].

Regarding the cellular inflammatory response after TBI, it is generally believed that the extravasation, migration and aggregation of neutrophils and macrophages are some of the main features(reference). These processes are regulated by cytokines, adhesion molecules, and chemokines secreted in the extracellular matrix[7]. In the damaged brain tissue, polymorph nuclear leukocytes adhere to the capillaries within a few minutes after TBI, and reach a peak of exudation within 24 hours of the acute phase; while T lymphocytes aggregate at 18 hours after injury and reached a peak at about 24 hours; Nuclear-macrophages begin to appear 36-48h after injury[38, 118]. Current research is still very controversial about the specific role of inflammatory cells in TBI. Many studies believe that inflammatory cells around the contusion can be caused by the release of myeloperoxidase, inducible NOS, MMPs, cells and chemokines. Reducing neutrophils can reduce the damage of the blood-brain barrier, the infarct area, prevent neuronal apoptosis, and promote the recovery of nerve function after trauma[60].

The role of inflammatory factors in secondary brain injury has been gradually confirmed. For example, IL-1β and TNF-α can promote the migration of neutrophils from the periphery to the brain and stimulate the release of proteolytic enzymes and oxygen. Studies have also shown that some cytokines can induce astrocytes to produce nerve growth factors[91] and anti-inflammatory factors[12], reducing the toxic damage caused by

excitatory amino acids, and promote neuronal differentiation and survival. Cytokines may be protective or toxic based on the amount and time or release. IL-1β, IL-6, and TNF-α, which represent pro-inflammatory factors, are expressed early followed by IL-8. The expression of chemotactic and adhesion factors represented by ICAM-1, and finally IL-4, IL-10, TGF-β and other anti-inflammatory mediators[64, 111]. After TBI, there are multiple cytokines signaling pathways that mediate inflammation, with different interactions in the cytoplasm or nucleus after activation. In addition, each signalling pathway can activate its own positive or negative feedback regulation mechanism, so that the response tends to be amplified or blunted[111]. These effects are different in various cell types, and regulation mechanisms in TBI remain to be fully investigated.

Long-term and delayed neuroinflammation in turn recruits' macrophages activates resident microglia and promotes astrocytes. The accumulation of macrophages and activated microglia in TBI survivors demonstrated progressive phagocytosis and sustained inflammation, years after injury [61].

1.1.5 The role of apoptosis in TBI

TBI results in an upregulation of apoptotic genes. Neurons, glial cells and endothelial cells can undergo apoptosis. There are many cellular and molecular processes involved when a cell undergoes apoptosis, like; increased excitatory amino acids (glutamate), increased ROS, mitochondrial dysfunction, energy failure and a deficiency in neurotrophic factors [128]. The apoptosis initiation signal after TBI could arise from both inside and outside the cell. The intracellular initiation signal is mainly triggered by mitochondrial dysfunction[98], however the extracellular initiation signal is mediated by the TNF receptor superfamily[104]. Mitochondria are the targets of a variety of pro-apoptotic signal transduction molecules and are also the integration sites of many cell death pathways. This pathway is mediated by members of the Bcl-2 family containing BH3 domains and is activated by intracellular death signals[103]. Bcl-2 family members mainly include pro-apoptotic and anti-apoptotic proteins. The former can release cytochrome C and apoptosis-inducing factors into the cytoplasm; the latter can inhibit this process by competing with the former on the surface of the mitochondrial membrane[102].

The extracellular apoptosis pathway is activated by the TNF/nerve growth factor receptor superfamily on the cell surface[105]. After TBI, these receptors activate neuronal apoptosis

signals by binding to corresponding ligands. TNF-α is an important cytokine, which has a special role in the TBI-mediated neuroinflammatory response[95]. It is barely overexpressed in the brain after mild head injury, but for severe head injury, it is significantly increased within 1-12 hours after injury[5]. After TBI, TNF-α is mainly expressed in neurons around the contusion, and a small part of it is expressed in astrocytes and microvascular endothelial cells. These enhanced expressions are important reasons for subsequent neurological damage[41].

In addition, to apoptosis, there are many processes involved in the pathophysiology of brain injury such as, autophagy[127], axon degeneration[53], mitochondrial dysfunction[121] and endoplasmic reticulum stress (ERS)[68].In addition, the above-mentioned mechanisms do not occur in isolation, but appear at the same time, and are interconnected to form a chain reaction of pathophysiology post TBI. Generally, the mechanism of secondary brain injury after TBI is complex. In addition to the above-mentioned mechanisms, epilepsy and depolarization of cortical transmission, demyelination and white matter loss, changes in cerebral blood flow, neurodegeneration and differentiation of neural stem cells have been observed widely after brain injury[77].

1.1.6 The clinical features and biological markers

For the clinical diagnosis, the preferred radiologic test in the emergency setting is computed tomography (CT): it is quick, accurate, and widely available. Follow-up CT scans may be performed later to determine whether the injury has progressed. On the other hand, the Glasgow Coma Scale (GCS) which is a neurological scale that can give a reliable and objective prognosis of the state of patients' consciousness. It is a scoring system based on verbal, motor, and eye-opening reactions to external stimuli. GCS has been used to classify TBI as mild (GCS $\geqslant$ 13), moderate (GCS 9-12), or severe (GCS $\leqslant$ 8)[56]. Mild, moderate, and severe TBI involve a spectrum of similar mechanical forces as well as partially overlapping pathophysiology. However, patients with these conditions often display disparate symptomology, and their diagnosis and management can entail distinct approaches[77].

With the development of modern biology, more and more studies have found that the types and severity of TBI are related to biomarkers, which can be detected in body fluids to further understand the stage of disease development[2, 124]. Biomarkers, such as proteins, and metabolites have been extensively explored in patients across the spectrum of TBI

severity. In particular, studies of protein biomarkers as a means for diagnosing, monitoring, and predicting the course of concussions has increased markedly over the past decade[3]. Here we briefly focus on 2 proteins with clinical approval. GFAP and NSE have demonstrated utility for discerning adult patients with TBI who may benefit from neuroimaging[107]. Protein biomarkers may require BBB disruption to migrate from cerebral spinal fluid (CSF) into blood. As a result, the sensitivity of protein biomarkers for TBI detection may be limited in individuals with mild TBI. Unlike protein biomarkers, small non-coding RNA might be more stable and more sensitive in the blood. Dependent on the phase post TBI, the expression of small non-coding RNA can vary. For example, miR-21 is expressed in the early stage of moderate TBI which may indicate the extent of neuronal damage[36], but mirR-155 is always expressed in the intermediate stage of moderate and severe TBI, which may indicate that there is neuroinflammation[46].

1.2 The general introduction and functional roles of circRNAs

Circular RNAs (circRNA) are a new class of regulatory RNAs originating from ‘‘head-to-tail’’ RNA back-splicing resulting from covalently closed continuous loops and are more stable compared to their linear counterparts[89]. CircRNAs are expressed from known proteincoding genes and consist of one or more exons. Products resulting from all of the basic types of alternative splicing of linear RNA can be found within circRNAs and some circRNAs contain exons that are not included in linear transcripts[88]. However, internal intron retention may lead to the production of circRNAs that contain sequences derived from both exons and introns (known as exon–intron circRNAs), and circular intronic RNAs (ciRNAs)[48].

Structure and location may determine its pathophysiological function. Based on current studies, it was found that circRNAs mainly functions as sponging miRNAs, RNA binding proteins (RBPs), coding small peptides and regulating transcription[106]. Firstly, circRNAs are important components in regulating post-transcriptional translation. Some of them are able to make miRNAs or ceRNA as response elements to inhibit the expression of target genes. For example, circRNA ABCB10 can sponge miR-670-3p to form a complex, which increases HMG20A expression to promote hepatocellular carcinoma progression[35]. Secondly, some circRNAs can bind the RBPs or directly interact with regulatory proteins. For example, during the process of the post myocardial infarction, circFndc3b can

modulate the miR-289-5p/FUS/VEGF-A axis. However when the miRNA binding locus was mutated, compared with wild type plasmid, it did not affect FUS and VEGF-A protein expression[35]. Thirdly, circRNAs can code small proteins and peptides. Compared with their linear host gene products, circRNAs encoded proteins or peptides have independent biological functions. For example, circAKT3, which encodes a 174 amino acid novel protein, can negatively regulate the RTK/PI3K pathway[114]. Finally, some studies have found that some special circRNAs, which are exon–intron circRNAs reside in the nucleus, where they can promote the transcription of their parental genes via interaction with the U1 small nuclear ribonucleoprotein or by positively regulating RNA polymerase II (Pol II)-mediated transcription[75]. These results prove that when the gene begins to be transcribed, the EIciRNA (exon-intron circRNA) generated from the gene will further promote the transcription of the gene. In general, circRNA regulates physiological and pathological changes through the above four modes.

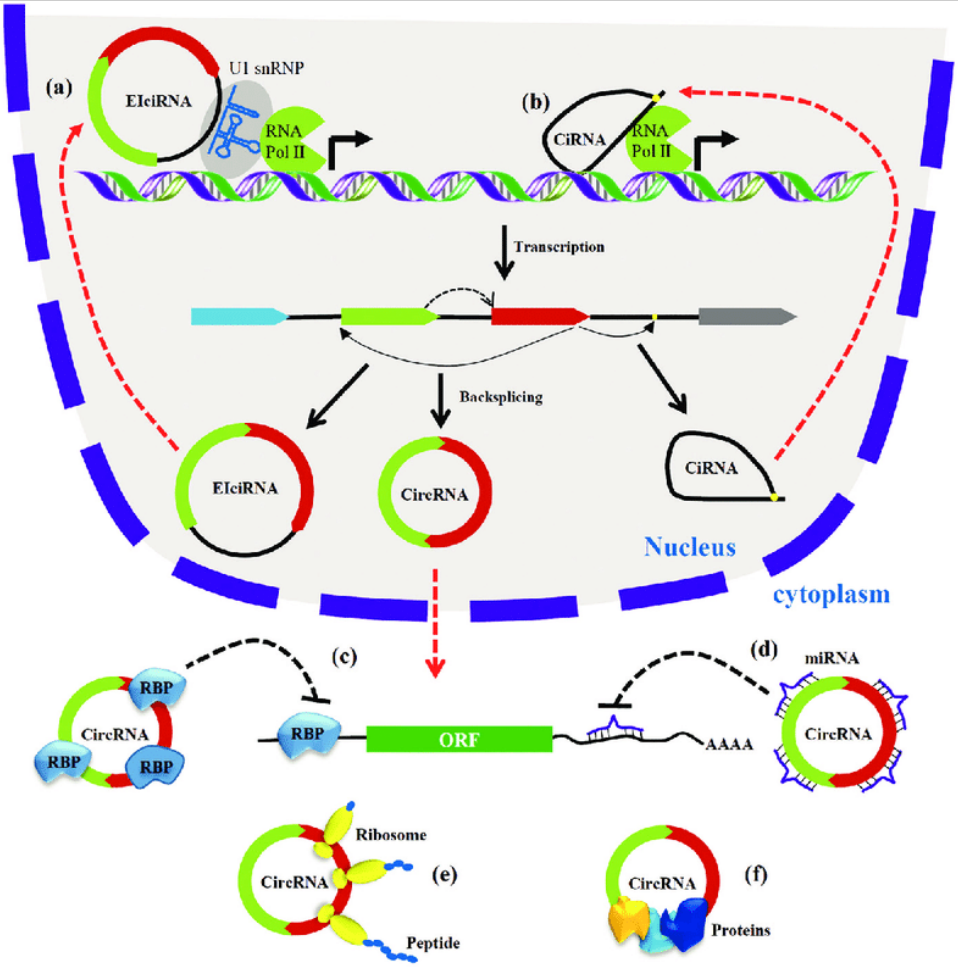

Figure 1. The main functions of the circRNA. CircRNA plays diverse roles by regulating transcription, sponging miRNAs and thereby derepressing miRNA-target mRNA translation, sponging RNA binding proteins (RBPs) et al. Reprinted from[20]with permission from Journal of Non-coding RNA Investigation.

1.2.1 General introduction of circRNA in Central Nervous System

CircRNAs are highly abundant, tissue-specific and evolutionarily conserved RNAs, and are widely expressed across many species [88]. Interestingly, circRNAs are not homogenously distributed throughout the nervous system but are differentially expressed in various brain regions and subcellular compartments, and at specific embryonic and postnatal stages[123]. Accumulating data suggest key roles for them in the central nervous system. Neuronal-expressed circRNA are dynamically modulated in neurons, both during differentiation and following bursts of activity. They might increase with age, and many of them are enriched in synapses[119]. For example, circDlgap1 showed about 20-fold increase in rats P30 when compared with E18, but the host gene Dlgap1 mRNA expression increased less than 4-fold, indicating a putative role of this circDlgap1 during synaptogenesis or when mature synapses have formed[69, 123]. In addition, there are many circRNAs whose levels change independent of their host linear transcript, suggesting that there may be a biological role for specific circRNA biogenesis. In gliomas, for example

the circMAPK4 can inhibits cell apoptosis via MAPK signalling pathway, but the host gene of circMAPK4, MAPK4, did not show significant difference between tissue with glioma and healthy controls. circMAPK4 can directly regulate phosphorylation levels of p38 to inhibit cell apoptosis to promote tumorigenesis[122].

1.2.2 The role of circRNAs in Neurological Diseases

Acute ischemic stroke (AIS) is a common neurological disorder and one of the major causes of permanent morbidity and disability worldwide. Due to a short time window and the side effects of recombinant tissue plasminogen activator, the efficacy of ischemic stroke thrombolytic therapy is limited[26]. However, since mature neurons are generally considered to be non-renewable cells, to rescue ischemic neurons in the brain from irreversible injury, the penumbra has become a top priority for treatment[112]. Over the years, neuroinflammation[90], autophagy[108], synapse plasticity[25] and other mechanisms have been reported to play critical roles in AIS pathogenesis[40].

Recent reports suggest that circRNAs play a vital role in the pathophysiology of AIS. Both in human patient blood samples as well as in the mouse tMCAO model, where the pathological progress of AIS is well established. Several circRNAs showed altered expression, which were suggested to modulate AIS pathology or served as a biomarker[133]. To investigate the potential involvement of circRNAs in stroke, Fangfang Wu et al established tMCAO mouse model of stroke, and performed a brain circRNA microarray. The results revealed that 5 of the 1178 circRNAs in the circRNA array were significant upregulated compared with sham group. For example, Circular RNA TLK1 can aggravate neuronal injury and neurological deficits via miR-335-3p/TIPARP. In fact, inhibiting circTLK1 expression can significantly decrease infarct volumes, attenuate neuronal injury, and improved neurological deficits. Furthermore, plasma of patients with acute ischemic stroke also showed significantly increasing levels of circTLK1[112]. In addition, circHECTD1 acts as an endogenous miR-142 sponge to inhibit miR-142 activity and regulate macrophages to activate astrocytes through autophagy[44] and circDLGAP4 can significantly attenuate neurological deficits and decrease infarct areas and blood–brain barrier damage in the transient middle cerebral artery occlusion mouse stroke model[4].

In human ischemic stroke patients, some studies identified that circRNAs were differentially expressed in blood according to stroke ethology. These studies reveal that circRNAs play a decisive role in ischemic stroke by regulating neuronal injury, astrocyte activation and blood-brain barrier damage[4, 112]. Taken together, these studies suggest that circRNAs modulate the gene expression resulting in ischemic stroke pathogenesis.

CircRNAs also have been found associated with neurodegenerative disease, such as Alzheimer's disease (AD)[65], Parkinson's disease (PD)[50], multiple sclerosis (MS)[49], and amytrophic lateral sclerosis (ALS)[82]. For example, In the APP/PS1 mouse model for AD, ciRS-7 were discovered that can reduce both the immature BACE1 which can reduce the abnormal splicing of ameloid precursor protein (APP), thereby reducing the production of amyloid beta (Aβ)[65, 92]. Yanjun Lu et al. reported that both circHDAC9 was reduced in Aβ-treated N2a cells and in 4-month-old APP/PS1 mice[62]. CircHDAC9 can was negatively correlated with miR-138 in Aβ-treated N2a cells and in 4-month-old APP/PS1 mice, abnormal APP processing and synaptic plasticity were enhanced by inhibiting miR-138 expression [17]. Moreover, ciRS-7 has been found to be associated with Parkinson's disease. Interestingly, ciRS-7 is mainly expressed in excitatory neurons, and it regulates the stability and/or transport of miR-7 which, through regulation of abnormal alpha-synuclein aggregates, contributes to neurodegeneration in PD, [45, 58, 131]. In addition, Errichelli et al reported that intervening with FUS, which is regulating gene expression in motor neurons, led to the overall down-regulation of circRNAs expression in mice [31]. These findings could have considerable implications for further research on circRNAs in ALS as mutations in FUS have been detected in ALS patients.

Although studies evaluating the role of circRNAs in neurological diseases are limited, the association of circRNA in several physiological and pathological conditions have proven the importance of these molecules[42]. Further evaluation of the regulatory mechanisms of circRNAs in neurological diseases may lead to development of novel treatment options.

1.2.1 CircRNAs as neurological disease biomarker

CircRNAs are promising biomarkers due to their stability, cell-specific expression patterns, and capacity for conditional expression. Although circRNAs are considered to be highly expressed in nerve tissue, they have been identified in various biofluids, including blood,

saliva, and plasma, and are also present in exosomes[17, 33]. Therefore, they have been proposed to serve as biomarkers for multiple illnesses including stroke, tuberculosis, rheumatoid arthritis, diabetes, and cancer. In stroke, Xiapei Peng et al. used a total of 160 AIS patients and 160 controls detected circHECTD1 expression in blood samples by RT-qPCR. In AIS patients, circHECTD1 expression was positively correlated with NIHSS score[44]. Additionally, analysis of peripheral blood mononuclear cells in patients with severe depression showed that after eight weeks of antidepressant treatment, hsa_circRNA_103636 showed significant differential expression, indicating that the circRNAs may be used as a therapeutic biomarker[19]. Although there is no clinically available circRNA kit for clinical testing. Identifying biomarkers of brain disease is important due to the inaccessibility of brain tissue for biopsy. In neurological diseases, such as TBI[115], AD[28], stroke[134], and ALS[81], the blood-brain barrier may be damaged, so that free circRNAs or vesicle-encapsulated circRNAs can escape from the brain and could be detected in bolalipids. Or Brain derived cells could release mediators to stimulate white blood cells to produce specific circular RNA. Therefore , it would be of interest to measure and correlate the concentration of circRNAs with disease progression.[132]

1.3 The aim of this study

Traumatic brain injury (TBI) is a major, lethal and highly disabling disease in modern society that is imposing substantial burdens on individual sufferers, their families, and society[84]. Although surgery-based comprehensive therapy has greatly improved the treatment of TBI, due to the accident and the complexity of the nervous system itself, surgery cannot completely solve the remaining problems, such as dyskinesia, epilepsy, and other TBI-related diseases[77]. circRNA is a type of endogenous noncoding RNAs and has become a new target for regulating physiological functions and mediating various neurological diseases. It is worth noting that the analysis of high-throughput sequencing results of circRNA showed that the expression of circRNA in rat, mouse, and human cerebral cortex and hippocampus showed abnormal changes after TBI[14, 115]. Circular RNA may be involved in various pathophysiological processes after TBI and may play a key role in secondary damage or complications of TBI.

1) As described above, the proper function of circRNA is essential for maintaining synaptic plasticity required for optimal neuronal function. In the pathological process of TBI, synapses will undergo three stages, namely; damage, functional degradation and remodelling. Which affects neurodegeneration and changes in memory function. The first purpose of this study was to identify the expression of synaptic-related circRNAs in hippocampus tissues in different disease stages using an experimental TBI model, to speculate its related functions.

2) Previous studies reported a disruption of excitatory synapses in the hippocampus of TBI mice compared to WT controls. This may be the cause for dyskinesia and memory impairment post TBI. Neurotrophic drugs are some of the classic drugs for the treatment of TBI, such as neurotrophic factors or monostatic gangliosides. These drugs have been used in clinical treatment of TBI patients, with promising efficacy. In the second part of this study, we will explore whether overexpression or knock-down of a chosen circRNA can effectively infect neurons (performed by intracerebral injection of an AAV2/9 expressing the circRNA of interest) As a read-out, behavioural analysis will be performed investigating the beneficial or detrimental effect of circRNAs in the experimental TBI model.

3) In the third part of this study, we will further prove the role of circRNA in different nerve injury models. We will investigate the effect of circRNA in the optic nerve injury model. The optic nerve belongs to the peripheral nerve that exits directly from the telencephalon, but the basic structure and treatment are similar to the central nerve.

In this study, we set out to use the mouse injury models, experimental blunt TBI and optic nerve crush together with brain tissues of patients, to investigate the role of circular RNA in TBI. With this experimental setting, we set out to explain the biological role of circRNA of neuronal preservation, synaptic remodelling, and memory repair after TBI. So, we decided to specifically focus on the mechanism of synaptic-related circRNAs in traumatic brain injury. It has proven that some circRNAs are therapeutic targets for movement and cognitive recovery after TBI. CircRNAs may be promising biomarkers for TBI diagnosis, treatment, and prognosis prediction. However, further research is needed to clarify the potential mechanism and therapeutic effect of circRNAs in TBI.

2 Materials and methods

2.1 Materials

2.1.1 Laboratory equipment

Item	Company
-80°C Deep freezer	Kaltis, Taiwan
-20°C Freezer	Kirsch, Germany
Cryostat	Leica, Germany
Desk centrifuge	VWR International GmbH, Germany
Disposable hypodermic needle 0.4 x 20 mm	B.Braun Melsungen AG, Germany
Disposable hypodermic needle 0.9 x 40 mm	B.Braun Melsungen AG, Germany
Disposable hypodermic needle 0.45 x 12 mm	Henke sass wolf, Germany
Excel 2013	Microsoft, USA
Fume cupboard	Wesemann, Germany
GraphPad Prism 6	GraphPad Software, USA
Image J	National Institutes of Health
LSM-710 Confocal laser scanning microscope	Carl Zeiss AG, Oberkochen, Germany
Magnetic hotplate stirrer	VWR International GmbH, Germany

Microwave oven	Severin, Germany
Microscope slides (Ground edges frosted)	VWR International GmbH, Germany
Microscope coverslips 24x50 mm	VWR International GmbH, Germany
Microscope coverslips 21x 26 mm	VWR International GmbH, Germany
Microscope slides folder	VWR International GmbH, Germany
Microtome blades	Feather, Japan
Mini microcentrifuge	Biozym, Germany
Mini vortex shaker	Greiner Bio-one GmbH, Germany
Perfusion tubing pump	Ismatec, Germany
Scalpel	Aesculap AG, Germany
Scales	Sartorius, Germany
Shaker	IKA® Werke GmbH, Germany
Sterile nitril gloves	B.Braun Melsungen AG, Germany
Tissue-Tek O.C.T compound	Sakura Finetek, Netherlands
Water bath	VWR International GmbH, Germany
Word 2013	Microsoft, USA

2.1.2 Plastic materials

Item	Company
15ml FALCON conical tube	BD Falcon Biosciences, Germany
50ml FALCON conical tube	BD Falcon Biosciences, Germany
24-well plate	Greiner Bio-one GmbH, Germany

48-well plate	Greiner Bio-one GmbH, Germany
96-well plate	Greiner Bio-one GmbH, Germany
Eppendorf tubes 0.5 ml	Eppendorf, Germany
Eppendorf tubes 1.5 ml	Eppendorf, Germany
Eppendorf tubes 2 ml	Eppendorf, Germany
Eppendorf tubes 5 ml	Eppendorf, Germany
Filter	Sartorius, Germany
Peel-A-Way® disposable plastic tissue embedding molds (22×22×20 mm deep)	Polyscience, Inc. U.S.A.
Pipettes tips	Sarstedt, Germany
Sarstedt serological pipettes 5 ml	Sarstedt, Germany
Sarstedt serological pipettes 10 ml	Sarstedt, Germany
Sarstedt serological pipettes 25 ml	Sarstedt, Germany
Syringe 1ml	BD Plastipak, Spain

2.1.3 Equipment for hippocampus injection

Item	**Company**
Active charcoal absorption filter	UNO BV, Netherlands
Bepanthen® wound and healing ointment	Bayer, Germany
Capillary puller PC-10	Narishige, Japan
Cotton-tipped applicator	Paul-Hartmann, Germany
Dumont vessel cannulation forceps	Fine science tools, Germany

Fine scissors	Fine science tools, Germany
Gas anesthesia head holder	David Kopf Instruments, USA
Gas exhaust unit	UNO BV, Netherlands
Glass capillaries 1mm	World precision instrument, USA
Heating pad	Stoelting, Ireland
Induction box for anesthesia	UNO BV, Netherlands
Microloader pipette tips	Eppendorf, Germany
Micro needle holder	Fine science tools, Germany
Picospritzer	Parker, USA
Prolene 7-0 suture thread	Ethicon, Germany
Sigma-delta isoflurane vaporizer	Penlon, UK
Stereotactic frame	Consultants GmbH D-40211, Germany
Vannas-Tübingen spring scissor	Fine science tools, Germany
Zoom stereo microscope for surgery	Olympus, Japan

2.1.4 Chemicals and drugs

Chemicals and drugs	Company	Reference number
Albumine Bovine Fract V (BSA)	Applichem Panreac, Germany	A1391
Temgesic ampullen Buprenorphine	Reckitt Benckiser Healthcare, UK	-
D(+)Sucrose	Carl Roth GmbH, Germany	4661.2
Distilled water	Fresenius Kabi, Germany	7151-5
Ethylenediaminetetraacetic acid (EDTA)	Applichem Panreac, Germany	A4892
Ethylene glycol	Carl Roth GmbH, Germany	6881.1

Fast green FCF	Sigma-aldrich Chemie GmbH, Germany	F7252-5G
Glycerol	Honeywell, Germany	15523
Hydrochloric acid (HCl)	Honeywell, Germany	35328
Meloxicam	Böhringer Ingelheim, Germany	-
Natriumhydrogenphosphat (Na2HPO4)	Carl Roth GmbH, Germany	P030.2
Ketamine	WDT, Germany	-
Paraformaldehyde (PFA)	Sigma-Aldrich Chemie GmbH, Germany	441244
Phosphate buffered saline (PBS) 1X w/o Ca^{2+}/Mg^{2+}	Gibco, Thermo Fisher Scientific, Germany	14190-094
Sodium chloride (NaCl)	Sigma-aldrich Chemie GmbH, Germany	31434
Sodium hydroxide(NaOH)	Carl Roth GmbH, Germany	6771.3
Triton-X-100	Sigma-Aldrich Chemie GmbH, Germany	T8787
Rompun (Xylazine)	Bayer, Germany	-
Tri-Sodium citrate	Sigma-Aldrich Chemie GmbH, Germany	71405

2.1.5 Antibodies for co-staining with BaseScope

Primary antibody	**Dilution**	**Company**	**Reference number**
Chicken anti-MAP2 antibody	1:200	Ecnro	CPCA-MAP2
Guinea pig anti-Iba1 antibody	1:200	SYSY	234 004
Mouse anti-GFAP antibody	1:200	Sigma	G3893

Guinea pig anti-VAChT antibody	1:200	SYSY	139105
Guinea pig polyclonal anti-RPBMS antibody	1:200	Abcam	ab152101
Secondary antibody	**Dilution**	**Company**	**Reference number**
Donkey anti-Guinea pig IgG (H+L) Alexa Fluor® 405	1:200	Abcam	ab175678
Donkey anti-chicken IgG (H+L) Alexa Fluor® 488	1:200	Biotium	20166
Donkey anti-mouse IgG (H+L) Alexa Fluor® 647	1:200	Life Technologies	A31571
Donkey anti-Guinea pig (H+L) Alexa Fluor® 633	1:200	Life Technologies	A21105
DAPI	1:1000	Thermo	62247

2.2 Methods

2.2.1 Animal model and husbandry

In total, 54 male B6-SJL WT mice were considered for this study (anima license number 1496). All procedures described were performed in accordance with the "3R" ethical rule for animal experimentation and to avoid unnecessary animal suffering. All experimental animals were housed at the animal research center in Oberberghof of Ulm University. All the animals were kept under standard conditions: 2-5 animals per cage, and were kept in temperature- and humidity-controlled rooms on a 12- hour: 12-hour light-dark cycle. Food and water were provided ad libitum.

2.2.2 Human brain sample collection

Patients were recruited among patients admitted to the department of neurosurgery

of Kaifeng Central Hospital Affiliated to Xinxiang medical University between January 2018 and January 2021. Computed tomography scan (CT) of the brain confirmed the diagnosis of TBI. Experienced neurologists determined the severity of patients' neurological deficits using the GCS within 1h of register in Sugary of Intensive Care Unit (SICU). Human Brain tissue samples came from 17 patients with traumatic brain injury (11 males, 6 females, age range 22.8-85.6 years, average age 54.0 years) and 17 patients with non-nerve injury diseases such as cerebral haemorrhage or aneurysm (Control group, 10 males, 7 females, age range 36.2-76.5 years, average age 58.3 years). The patient came from the department of neurosurgery of Kaifeng Central Hospital Affiliated to Xinxiang medical University. These studies are supervised by the Kaifeng Central Hospital or Xinxiang medical university Human Ethics Committee and strictly comply with relevant regulations. The patients in the TBI group all have typical clinical manifestations and CT characteristics. The demographic and clinical characteristics of patients enrolled in the study are provided in Table 1.

Table 1. Details of the 17 TBI patients

Case	Age (years)	Sex	Cause of injury	Duration (h)	Cause
1	46.1	M	Fall	3.2	Brain + multiple injuries
2	63.9	M	Motor vehicle accident	3.5	Brain injury
3	49.1	F	Motor vehicle accident	5.5	Brain injury
4	49.5	M	Motor vehicle accident	4.2	Brain injury
5	53.3	F	Fall	3.5	Brain + multiple injuries
6	67.5	M	Motor vehicle accident	6.5	Brain injury
7	65.2	M	Fall	3.8	Brain + multiple injuries
8	57.5	M	Motor vehicle accident	5.2	Brain injury
9	85.6	M	Motor vehicle accident	100	Brain injury
10	23.8	F	Motor vehicle accident	2.0	Brain injury
11	22.8	F	Motor vehicle accident	3.0	Brain injury
12	54.6	M	Fall	5.2	Brain + multiple injuries
13	65.5	M	Motor vehicle accident	60	Brain + multiple injuries
14	60.5	F	Motor vehicle accident	6.2	Brain injury
15	65.7	M	Fall	5.2	Brain + multiple injuries
16	48.9	F	Motor vehicle accident	58	Brain injury
17	38.9	F	Motor vehicle accident	101	Brain injury

The diagnosis meets the following conditions:

(1) Have clear history of TBI and GCS ≤8.

(2) No family history of nervous system diseases (such as stroke, epilepsy etc.)

(5) The patient or the guardian agrees that the surgical specimen is used for scientific

research and signs the informed consent.

Control group:

(1) No history of brain injury.

(2) Patients without with nerve injury diseases.

(3) The patient or guardian agrees that the surgical specimen is used for scientific research and signs an informed consent.

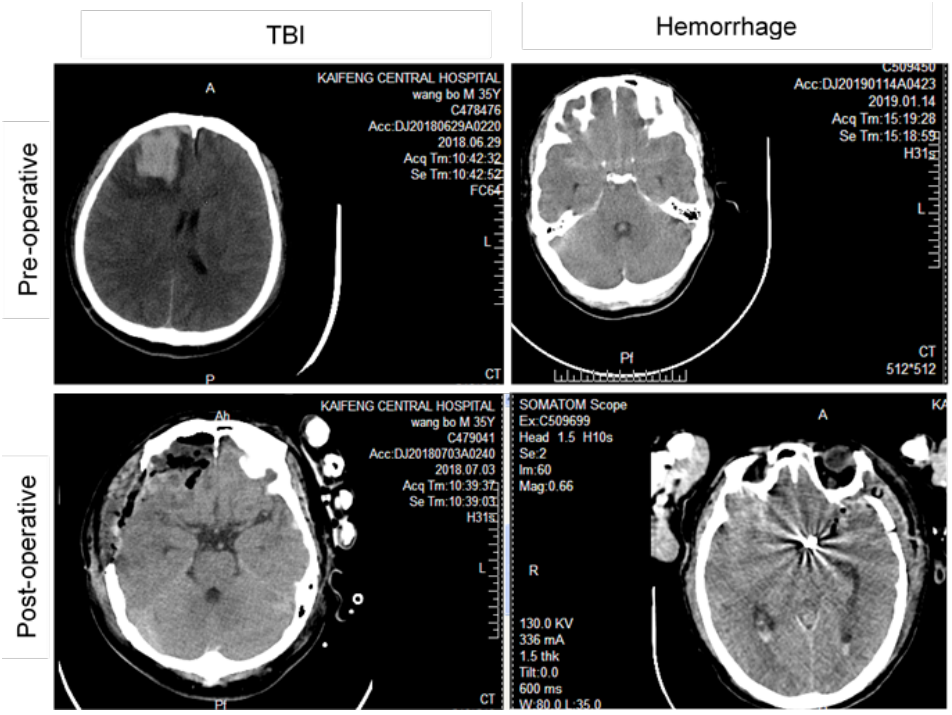

Figure 2. The CT images of surgical specimens for patients with TBI or non-TBI. For patients with TBI, we select the core part of brain injury in patients with traumatic brain injury (CT shows high-density signal before surgery, CT shows defect signal after surgery); for patients with hypertensive cerebral haemorrhage or aneurysm, we choose normal brain tissue of the sinus tract that enters the bleeding site as our control group (post-operative CT showed low-density signal).

2.2.3 RNA isolation and qRT-PCR

RNA isolation: Add 1 ml QIAzol Lysis Reagent per 100 mg tissue. Place the tip of the Tissue Raptor disposable probe into the QIAzol Lysis Reagent and operate the Tissue rotor at full speed until the tissue lysate is uniformly homogeneous. Place the tube containing the homogenate on the benchtop at room temperature (15–25°C) for 5 min. Add 0.2 ml chloroform per 1 ml QIAzol Lysis Reagent and shake it vigorously for 15 s. Place the tube containing the homogenate on the benchtop at room temperature for 2–3 min. Centrifuge at 12,000 x g for 15 min at 4°C. Transfer the upper, aqueous phase to

a new tube. Add 0.5 ml isopropanol per 1 ml QIAzol Lysis Reagent. Mix thoroughly by vertexing. Place the tube on the benchtop at room temperature for 10 min. Centrifuge at 12,000 x g for 10 min at 4°C. Carefully aspirate and discard the supernatant. Add at least 1 ml of 75% ethanol per 1 ml QIAzol Lysis and centrifuge at 8000 x g for 5 min at 4°C. Remove the supernatant completely, and briefly air-dry the RNA pellet. Redissolve the RNA in an appropriate volume of RNase-free water. Detection of RNA quality: The total RNA extracted was measured by UV spectrophotometer NanoDrop 2000, and the ratio of A260/A280 should be between 1.8-2.0. In addition, the integrity of RNA was analysed by 1.5% agarose gel electrophoresis. Generally, the total RNA with good quality clearly shows three bands of 28s, 18s and 5s, and 28s: 18s is about 2: 1.

Ribonuclease-R (RNase R) Treatment: RNA purified from TBI mouse hippocampus was treated with RNase R (Epicentre RNR07250) at concentrations of 10 U of RNase R/μg of total RNA. A non-treated sample served as control. The reaction mix that included RNA (2 μg of total RNA), 10x RNase R Buffer, and RNase R was incubated at 37 °C for 30 min and the resulting RNA was subsequently purified continuing with the isopropanol step of RNA isolation[74].

cDNA synthesis: Reverse transcription was performed with 0.75μg RNA or 12ul RNA with or without RNAse R using reverse transcriptase (Promega), RNase Inhibitor (RiboLock, Thermo Scientific), dNTPs (genaxxon) and random hexamers (Biomers). RNA (1ug RNA diluted in RNAse free dH20, total volume of 40ul) and 5ul random hexamers were desaturated by incubating for 10min at 75℃. The reverse transcriptase master mix (12ul RT buffer, 2ul dNTPs, 0.5ul RNAse inhibitor and 0.5ul reverse transcriptase) was added on ice and incubated for 45min in a waterbed at 45℃. A final incubation of 3min at 95℃ was performed. The samples were stored at -20℃

MiRNA cDNA synthesis: Reverse transcription was performed with 2μg RNA miScript II RT kit (Qiagen), 5×miScript Hispec buffer; 10×miScript Nucleics Mix; Rnase-free water; miScript Reverse Transcriptase Mix; up to 20ul on ice, water bath reaction at 37 ℃ for 60 min and heat at 95 ° C for 5min to stop the reaction, then place on ice and store at -20 ° C.

Quantitative RT-PCR: qPCR was performed on the Light Cycler 480II (Roche) with the Power PCR TB green PCR master mix (Takara). 2µl of cDNA was used in a total volume of 10µl (3µl primer mix and 5µl of TB green) in a 96-well plate, all samples were duplicated and the housekeeping gene GAPDH was used as a control (for the primer sequences see table 2). The CT values obtained from the lightcycler were calculated with the $2^{-\Delta\Delta Ct}$ formula.

Table 2. Primer list

Primer	Sequence
mmu-circ-0001679 (circKlhl2-F-1)	5´- AGGAGAACGTGCAGATGCACAA -3´
mmu-circ-0001679 (circKlhl2-R-1)	5´- TTCATGTGCCAGGGGTTCAC -3´
mmu-circ-0000679 (circDlg1-1-F)	5´- TTCCACATAGGGAGCAACC -3´
mmu-circ-0000679 (circDlg1-1-R)	5´- TTCTAAACACACACTGTTCACCG -3´
mmu-circ-0006189 (circDlg1-2-F)	5´- AAACGAAGCTTCTTCTCAATCTG -3´
mmu-circ-0006189 (circDlg1-2-R)	5´- AAATGGGTGAGTACCTGGCTG -3´
mmu-circ-0000491 (circHomer1-F-1)	5´- TTCCACATAGGGAGCAACC -3´
mmu-circ-0000491 (circHomer1-R-1)	5´- TCTTCTTTGTGTTCGGGTCA -3´
mmu-circ-0000811 (circDlgap1-1-F)	5´- CCCAGAAGACATGTCATCTTGC -3´
mmu-circ-0000811 (circDlgap1-1-R)	5´- CTGTGCTACTCTGGGCTGTG -3´
mmu-circ-0010603 (circNlgn1-F)	5´- TGCTTCCTGTGTGGTTCACT -3´
mmu-circ-0010603 (circNlgn1-R)	5´- GTGGGTCTATATCCATCTTCAGTT -3´
mmu-circ-0000810 (circDlgap1-2-F)	5´- ATTGGGATACAGGTGGACGATG -3´
mmu-circ-0000810 (circDlgap1-2-R)	5´- TGCAAGATGACACACTTCTCTTC -3´
mmu-circ-0006522 (circGrin2a-F)	5´- CTGCCGCATCTTCCATGTTG -3´
mmu-circ-0006522 (circGrin2a -R)	5´- CGTGGATGTCGGATCTGGTG -3´
mmu-circ-0001530 (circGrin2b -F-1)	5´- CCTGAGTGACAAGAAGGTGGG -3´
mmu-circ-0001530 (circGrin2b -R-1)	5´- GGTGCCTCCTCCAAGGTAAC -3´
mmu-circ-0001531 (circGrin2b -F-2)	5´- CATGCTGTCCGAACACAGTT -3´
mmu-circ-0001531 (circGrin2b -R-2)	5´- TGGAGGACTCATCCTATTCAGC -3´

mmu-circ-0000379 (circAkap6-F-1)	5´- ATCTCATTGAAAGGAGACTCTGAA -3´
mmu-circ-0000379 (circAkap6-R-1)	5´- ATTCCAGGGCATCCTCACTC -3´
mmu-circ-0000154 (circAkap7-F-1)	5´- CCTTCCAAGGGATTGGCACT -3´
mmu-circ-0000154 (circAkap7-R-1)	5´- AGTTTTCCTGCTATCTCCAGG -3´
mmu-circ-0000153 (circAkap7-F-2)	5´- TTCCATCGTGATCGGAAAACT -3´
mmu-circ-0000153 (circAkap7-R-2)	5´- CGGCATGTCTGTCAGGGAA -3´
mmu-circ-0004882 (circHomer1-F-2)	5´- TTCCACATAGGGAGCAACC -3´
mmu-circ-0004882 (circHomer1-R-2)	5´- TCTTCTTTGTGTTCGGGTCA -3´
mmu-circ-0000378 (circAkap6-F-2)	5´- AGAGGCAAATCAAACGGCAA -3´
mmu-circ-0000378 (circAkap6-R-2)	5´- TCAACTTAAAGCTCTTGGGGCT -3´
mmu-circ-0000703 (circNcam2-F)	5´- ATCCCATGGAGGTGTGCCTA -3´
mmu-circ-0000703 (circNcam2-R)	5´- GGCCATCCGGACTTTTGAAC -3´
mmu-circ-0000810 (circDlgap4-F)	5´- AGGGATGGCTACTGGTTCCT-3´
mmu-circ-0000810 (circDlgap4-R)	5´- GCATGATGAACCTTCTTCAGAGA -3´
mmu-circ-0008589 (circRims1 -F)	5´- TGATGTGTCCGCCATTTCCA -3´
mmu-circ-0008589 (circRims1-R)	5´- ACTACTAAGCTCGCTGATCCTG -3´
mmu-circ-0000132 (circRps6kc1-F)	5´- GATTACCTGGAGAAGGCAGGG-3´
mmu-circ-0000132 (circRps6kc1-R)	5´- CCACACAATTATCTTGTACACCTT -3´
mmu-circ-0000091 (circStx6 -F)	5´- CTCACATGACCAGTGAGAGGT-3´
mmu-circ-0000091 (circStx6-R)	5´- TGGTGGTCCAGTCGATTTCT-3´
mmu-circ-0000870 (circKcnn2-F)	5´- CCAGGAACTGTGCTCTTGGT -3´
mmu-circ-0000870 (circKcnn2-R)	5´- CCACCATGAATAACTTTCACAAGC -3´
mmu-circ-0007052 (circSlc8a1-F)	5´- CTCGGTGCCAGCAAAACAAT-3´
mmu-circ-0007052 (circSlc8a1-R)	5´- CTCACTCATCTCCACCAGACG -3´
mmu-circ-0000372 (circStrn3-F)	5´- TAGTGACTGCAGAAGATGGTGA -3´
mmu-circ-0000372 (circStrn3-R)	5´- ATGCAATCCGTGCCCCATTC -3´
mmu-circ-0008828 (circAls2-F)	5´- CTTGCTTTGAAGTGCTTGGAT -3´
mmu-circ-0008828 (circAls2-R)	5´- CAACTCATGGAGACTGGCGA -3´
mmu-circ-0001807 (circMyo5a-F)	5´- AATGCCTACAGTGGCCAGAAC -3´

mmu-circ-0001807 (circMyo5a-R)	5′- GGCAAACTTGCCATTTGCTTGT-3′
mmu-circ-0008278 (circCacna1e-F)	5′- TGGTCCTTAGTGGGATGGCT-3′
mmu-circ-0008278 (circCacna1e-R)	5′- TTCCTTGTCGGTTCCTGCTC-3′
hsa-circ-0071347 (circKLHL2-F)	5′- AGGTGAGATGAGTGAGAGCC-3′
hsa-circ-0071347 (circKLHL2-R)	5′- CTGGGCAGTGTTTTTCGGTA-3′
mmu-Klhl2-F	5′- CCGAAGAAGCACACTTGGAG -3′
mmu-Klhl2-R	5′- GATAGACCTGTGCTGCCGTC -3′
hsa- KLHL2-F	5′- CGGCCCCAGATTCTCTTTGT-3′
hsa-KLHL2-R	5′- CACTGGGCAGTGTTTTTCGG -3′
hsa-circ-0104975 (circGRIN2A-F)	5′- GCACCCGATCCGACGTCTA -3′
hsa-circ-0104975 (circGRIN2A -R)	5′- TGTGGTCTTGACGAAGCTGA -3′
mmu-Grin2a-F	5′- TGTTGAAAATGTGACCCTGCC-3′
mmu- Grin2a -R	5′- AAGGGGTTCCGGTTCATTGG -3′
hsa-GRIN2A-F	5′- AGCAGAGCTACCACGTTCAC-3′
hsa-GRIN2A-R	5′- TGTGGTCTTGACGAAGCTGA -3′
hsa- GAPDH-F	5′- AACGTGTCAGTGGTGGACCTG -3′
hsa-GAPDH-R	5′- AGTGGGTGTCGCTGTTGAAGT -3′
mmu-Bdnf	5′-ACCATAAGGACGCGGACTTG-3′
mmu-Bdnf	5′- GAGTAGAGGAGGCTCCAAAGGC -3′
mmu-U6	5′- CTCGCTTCGGCAGCACA-3′
mmu-miR-30a-5p	5′- TGTAAACATCCTCGACTGGAAGAA-3′
mmu-miR-30d-5p	5′-GTAAACATCCCCGACTGGAAGAA-3′
mmu-miR-34a-5p	5′-TCAGCAAGTATACTGCCCTAAA-3′
mmu- miR-376b-3p	5′- GTCACAGAGGAGAACGTGCA-3′

2.2.4 Cell culture and transfection

Neuro 2a and HEK 293T cells were both stored at department of neurology, Ulm university. The cells were cultured in Dulbecco's modified Eagle's medium (DMEM,

Gibco, USA) containing 10% fatal bovine serum (FBS, Gibco, USA) in a 37 °C incubator with a 5% CO2 humidified atmosphere. For the transfection, the cells were seeded 24 hrs before at a confluency of 40–60%. SiRNA (10nM) and plasmids (2.5µg) was performed by transfecting Neuro2a cells using Lipofectamine 2000 (Thermoscientific, Aalst, Belgium) and HEK 293T cells using PEI (Polyethylenimine). The cells were transfected on the day of subculturing in 2mL of culture medium per well of a 6-well cell culture plate, according to the manufacturer's instructions. RNA or protein extraction was performed at 24-72 h post-transfection.

2.2.5 Recombinant adeno-associated viruses produce AAV (rAAV) vectors

Adeno-associated viruses vector construction: The plasmids pAAV-U6-GFP-AMP with circKlh2 shRNA, pAAV-CMV-GFP-AMP with circKlh2 overexpression, and their control (Con) sequences were purchased from BersinBio and inserted into Adeno-associated viruses. For the cloning of vectors for AAV production, the following target sequences were used for RNAi: shRNA-circKlhl2 5'-CGTGCAGATGCACAAAGCA-3'and OE-circKlhl2 full sequence. Adeno-associated virus (AAV) vector construction. Three AAV vectors (AAV2/9 serotype), AAV-GFP-Con, AAV-GFP-shRNA-circKlhl2, and AAV-GFP-OE-circKlhl2, were constructed and packaged by BersinBio, China, and detected by IRES expression. All chemo genetic vectors suspension was injected at the titter of 10×10^13 genomic copies per µl [18, 54].

Table 3. Primers of the rAAVs

IRES: internal ribosome entry site

Primer	Sequence
IRES forward primer (IRES-F)	5´-TGGCTCTCCTCAAGCGTATT -3´
IRES reverse primer (IRES-R)	5´-CCTCACATTGCCAAAAGACG -3´

2.2.6 Hippocampus injection and TBI operation

The experiments were approved by the Ulm University veterinary and animal experimentation service and by the Regierungspräsidium Tübingen under the license number 1469. B6-SJL WT male mice, P35-45, underwent hippocampus injection. All the

intraspinal hippocampus injection procedures were done in the operating room of the animal research centre in Oberberghof of Ulm University. Mice were administered buprenorphine (0.01 mg/kg, subcutaneous injection) and meloxicam (1.0 mg/kg, subcutaneous injection) 30 min prior to the surgery. Mice were put into a stereotaxic frame in arched prone position and supplied with continuous 4% sevoflurane anaesthesia (in 96% oxygen at 800 ml/min). Mice eyes were covered with Bepanthen® wound and healing ointment, and the fur was removed with the blade. Mice were microinjected with either a circControl-GFP, circKlhl2-overexpression-GFP, or circKlhl2-shRNA-GFP Adeno-associated viruses (1µl of 1×10^13 viral genome/µl) at the following microinjection coordinates: 2.0 mm behind the bregma and 1.5 mm lateral from the sagittal midline, at a depth of 1.6mm from the skull surface. For virus delivery, a total of 1µl of viral suspension (Table 4 and Table 5) was injected within a pulled-glass capillary coupled to a Picospritzer-III microinjection dispense system at 8-10 msec pulses. The Fast-Green visible dye, used to visually monitor the injection, is easily washed away in PBS and does not interfere with the imaging procedures. An injection was performed over a span of 10 min (at 0.1µl/min). The capillary was kept in place for 10 more min after injection to prevent back flow of the viral suspension. After removing the capillary, and skin were stitched with Prolene 7.0 surgical thread sequentially. The animals were then transferred to a single cage with facilitated access to water, food and heating system for recovery. After recovering from the anaesthesia, animals were sent back to the animal room, housed in the original groups and home cages. Mice were monitored for eventual neurological impairment and were administered buprenorphine (0.05 mg/kg, subcutaneous injection, three times per day) and meloxicam (1.0 mg/kg, subcutaneous injection, once per day) for the following three days after surgery. To evaluate the effects of circKlhl2 on the TBI mouse model, mice were divided into the following six groups 4 weeks after AAV microinjection.

Traumatic brain injury model: B6-SJL WT male mice, 30 days post hippocampus injection (p65-75), underwent closed head weight drop TBI (according to Flierl et al. 2009). Buprenorphine (0.1mg/kg by subcutaneous injection) was administered 20 min before anesthetizing the mice with sevoflurane (5% in 95% O2). Mice were kept under sevoflurane anaesthesia during the procedure. The scalp was incised in the midline to expose the skull before positioning the mice in the weight-drop apparatus. The impactor was placed in the centre of the right parietal bone and a weight of 120 grams

was dropped from a height of 45cm and the distance of the impactor at 2.5mm (moderate). Under these conditions, neither bone fracture nor intraparenchymal haemorrhage was observed.

After the procedure, animals were treated with 100% O2 until restoration of spontaneous breathing (between 5 and 25 seconds) while the apnoea time was monitored. The skin was then sutured with Prolene 6.0 surgical thread. The animals were transferred to a separate cage with water and food ad libitum. Buprenorphine was administered every 8h for a total of 24h. The mice were checked daily, using a score sheet developed for TBI with fixed termination criteria (severe weight loss (> 15%), severe pain, severe behavioural deficits (decreased locomotion, convulsions, stupor), and intracerebral haemorrhage in consequence of TBI) to avoid unnecessary suffering. Efforts were made to minimize animal suffering and reduce the number of necessary animals, strictly adhering to the "3R" guidelines.

Table 4. Preparation of 1% Fast Green solution

1% Fast Green solution (10 ml)	
100 mg	Fast Green
10 ml	Distilled water

Table 5. Preparation of Viral suspension

Viral suspension (1 µl)	
0.5 µl	Viral solution
0.5 µl	1% Fast Green solution

2.2.7 Behavioural analysis

Y maze: To determine spontaneous alternation behaviour, we tested the mice in a Y-maze with 40 cm long, 10 cm wide and 20 cm high arms with 120° angles. Mice were tested individually, with each mouse placed in the centre square facing one of the corners and away from the researcher. Each mouse received one trial during which it was placed at the end of one of the three arms and allowed to explore the maze for 8

min on after TBI at the timepoints 3, 7,10 and 14 days. A video camera mounted above the maze recorded the movements of the mice for analysis. The arm entries were recorded, and the percentage of alternations was calculated with the viewer III software: The percent of spontaneous alternation (measure of spatial working memory) was measured.

Open Field Test: An open field test (OFT) was used to assess athletic ability and anxiety-like responses during the exploratory behaviour of mice. Mice were individually placed in the centre of an open field (40 × 40 × 40 cm) and allowed to explore freely for 10 min. Total distance, velocity and time spent in the centre or borders and entry times were recorded and analysed using viewer III software tracking system.

The novel location and object recognition test (NOR): a non-force driving and spontaneous memory test, was performed. Before training, each mouse was allowed to habituate to the test space (40 × 40 × 40 cm) for 10 min. During the training phase, the mouse was placed in the space with two identical objects (labelled as A and B respectively), one in each of two corners, and allotted 10 min for exploration. 1 hour later, the mouse was tested using the same procedure except that one object (B) was moved to a new position in the area, and the mouse was allowed to explore for 10 min. Exploration time was recorded as an indicator of spatial memory. 1 hour later, the mouse was tested using the same procedure except that one object (A) had been replaced with a novel object (C), and the mouse was allowed to explore for 10 min. Exploration time was considered to have started when the front paws or nose touch the objects and was analysed as the investigating time= T novel / (T novel + T familiar) and discrimination index (DI), DI = (T novel- T familiar / (T novel + T familiar).

2.2.8 Mouse perfusion and brain dissection and fixation

After waiting for 30 days of virus expression and receiving the TBI operation 7dpi and 14dpi after the final behaviour experiments, then the mice was perfused by intracardial injection to the left ventricle. Briefly, animals were terminally anesthetized with anaesthesia solution (Table 6). By using a peristaltic pump, the mice were transcranial perfused with 2 ml/g cold PBS 1X containing EDTA (Table 7, Table 8, and Table 9) followed by 2.5 ml/g of 4% PFA solution (Table 10). After removing all organs in the thoracic and abdominal cavity, the whole bilateral vertebral lamina was continuously

cut off to expose the whole brain. The brain was then carefully and quickly extracted and post-fixed in 4% PFA solution at 4˚C for 18 hours. Thereafter washed in PBS and cryoprotected in 30% sucrose (Table 11) at 4℃ for 36 hours. The brain was then isolated, embedded in a disposable tissue embedding mold (22×22×20 mm) in O.C.T., and snap-frozen by dry ice.

Table 6. Preparation of Anesthesia solution

Anesthesia solution (5 ml)	
3500 µl	0.9% Saline solution
1250 µl	Ketamine
250 µl	Xylazine

Table 7. Preparation of PBS 10X

PBS 10X (1000 ml)	
14.4 g	Na2HPO4
2.4 g	KH2PO4
80 g	NaCl
2 g	KCl
fill up to 1000 ml with	Distilled water
Adjusted to pH 7.4	1M HCl or NaOH

Table 8. Preparation of PBS 1X

PBS 1X (1000 ml)	
100 ml	PBS 10X
900 ml	Distilled water

Table 9. Preparation of 5 mM EDTA in cold PBS for perfusion

5mM EDTA in cold PBS (1000 ml)	
10 ml	0.5M EDTA
990 ml	PBS 1X

Table 10. Preparation of 4% PFA

4% PFA (100 ml)	
4 g	PFA
fill up to 100 ml with	PBS 1X
Adjust pH to 7.4	1M HCl or NaOH

Table 11. Preparation of 30% Sucrose

30% Sucrose (500 ml)	
150 g	Sucrose
fill up to 500 ml with	PBS 1X

2.2.9 Cryostat sections preparation

After snap-freezing and embedding, samples were transferred to the cryotome machine at -15 ℃. Each frozen sample was taken out from the tissue embedding mold and was fixed on a sample tray. 40 µm-thick cryostat sections were cut and serially collected in a 24-well plate containing PBS 1X for free-floating immunohistochemistry staining.

2.2.10 BaseScope and immunofluorescence staining

BaseScope is one product single-molecule in situ mRNA hybridization for circRNAs and performed according to manufacturer instructions (ACDBio, BaseScope) For the mouse sections BaseScope, sections were washed with 1× PBS for 2 h and then mounted with PBS on the slides. Air dry the slides for 15 min at RT and stored them overnight at -80℃. On the day of performing the BaseScope assay washed the slides with 200 ml 1×PBS in a Tissue-Tek slide rack for 5 min while the rack up and down to remove OCT. Baked the

slides for 30min at 60℃, and post-fix the slides by immersing them 4% PFA in 1×PBS 5 min at 4℃. After removing the slides from 4% PFA, immersed them in 50% EtOH for 5 min at RT and then took out, immersed them in 70% EtOH for 5 min at RT and then took out, and immersed them in 100% EtOH for 5 min at RT and repeated the last step once. Removed the slides from 100% EtOH and let them air dry for 5 min at RT. Prepared 350 mL fresh 1×Target Retrieval in a beaker. Covered with foil, bring a mild boil, and maintained uniform boiling at 99-100℃.Do not boiled more than 30 min before use. Put the slides in the boiling Target Retrieval solution and kept them in the solution for 5 min only and immediately transferred the hot slide racked to a staining dish containing distilled water. Washed slides in distilled water by moving the racked up and down 3-5 times and repeated with fresh distilled water. Rinsed slides in fresh 100% EtOH by moving the racked up and down 3-5 times and let them air dry. Drawed2-4 times around the tissue using the hydrophobic barrier pen. Let the barrier dry completely overnight at RT. Pre-warm the HybEZ Oven to 40℃ at least 20 min before use and removed circRNA probe and AMP 1-8 reagents from refrigerator before use, at least 30min at RT. Added 2-4 drops Hydrogen Peroxide to each section for 10 min at RT, and used enough solution to completely cover the sections. Then washed slides 3–5 times by moving up and down in the distilled water. Added about 4 drops per slide of the circKlhl2, negative and positive control probe to entirely cover each section, and inserted into the oven for 2 h at 40°C. Then, Removed the tray from the oven and removed the slide rack and washed slides in 1X Wash Buffer for 2 min at RT. Agitated slides by moving the slide racked up and down in the dish and repeated it. Added about 4 drops per slide of AMP 1 to entirely cover each section, and inserted into the oven for 30 min at 40°C. Then, Removed the tray from the oven and removed the slide rack and washed slides in 1×Wash Buffer for 2 min at RT. Agitated slides by moving the slide racked up and down in the dish and repeated it. Amp 2 to 8 were added and washed in the same manner with different incubation times: AMP 2 was incubated 30 min at 40°C; AMP 3 was incubated 15 min at 40°C; AMP 4 was incubated 30 min at 40°C; AMP 5 was incubated 30 min at 40°C; AMP 6 was incubated 15 min at 40°C; AMP 7 was incubated 30 min at RT; AMP 8 was incubated 15 min at RT. Prepare sufficient RED working solution per section by using a 1:60 ratio of BaseScope™ Fast RED-B to BaseScope™ Fast RED-A. Used the Fast RED-B solution within 5 min and mix well. Pipetted about 120 µL RED solution onto

each tissue section and seal tray and incubated for 10 MIN at RT. To remove the RED working solution from the slides, immediately inserted the slide into tap water and repeat again.

The co-immunostaining procedure was performed soon after as follows: the sections were blocked for 1 h in 10% BSA (Table 12), 0,3% Triton (Table 13) and 1×RNase inhibitors in PBS with Blocking buffer (Table 14) and incubated overnight with primary antibody (mouse anti-GFAP, 1:200 [abcam], chicken anti-MAP2, 1:200 [Encor] and guinea pig anti-IBA1, 1:200 [synaptic systems]). The Slides were washed 3 x 30 min and incubated with secondary antibody (Donkey anti-mouse 405, 1:500 [Invitrogen]; Donkey anti-chicken 647 and Donkey anti-guinea pig 568, 1:500 [Invitrogen]). After the last round of washing (3x30 min in PBS), the coverslips were mounted using Fluorogold prolong antifade mounting medium (Invitrogen). The mouse circKlhl2 probe designed form ACDBio company, and the probe sequence span Exon2-4. (ACDBio, BaseScope).

After washing, preparing one microscope slice and one coverslip for mounting the sections. The sections were mounted by removing access PBS and adding Prolong Gold antifade mounting medium on the slide and placing a coverslip on top. Samples were stored overnight to dry and subsequently imaged. The remaining sections were be stored in Cryoprotectant solution (Table 15) at -20℃.

Table 12. Preparation of 10% BSA

10% BSA (100 ml)	
10 mg	Albumine Bovine Fract V
fill up to 100 ml with	PBS 1X

Table 13. Preparation of 10% Triton solution

10% Triton solution (50 ml)	
5 ml	Triton-X-100
45 ml	PBS 1X

Table 14. Preparation of Blocking buffer

Blocking buffer (6.67 ml)	
2000 µl	10% BSA
200 µl	10% Triton solution
4466.67µl	PBS 1X

Table 15. Preparation of Cryoprotectant solution

Cryoprotectant solution (100 ml)	
50 ml	PBS 1X
30 ml	Ethylene Glycol
20 ml	Glycerol

2.2.11 Image Acquisition and analysis

The images were acquired in 1024x1024 pixel 12-bit format, using a Leica DMi8 microscope, equipped with an ACS APO 40x oil objective. Imaging parameters were set in order to obtain signals from the stained antibody or circRNA while avoiding saturation. In order to avoid fluorescence cross-bleed, all fluorescent channels were acquired independently. Per hippocampus, 4 regions were imaged (DG, CA1, CA2 and CA3). Optical stacks composed of 15 (for Fluorescence in Situ mRNA Hybridisation) 1µm stacks were obtained and imported in ImageJ. Confocal stacks (10 optical sections each) were collapsed in maximum intensity projection pictures. For Fluorescence In Situ Basescope Hybridisation, single-molecules of circRNA per one region were counted manually by an operator blind to the treatment groups. After all the sections were acquired, images were then deconvolved in an Image J software for analysis.

2.2.12 Statistics

Data analysis for the initial screening (fig. 4) was performed using the IBM SPSS software suite, using a two-way Multivariate ANOVA (and Wilk´s λ parameter) since the experimental design included multiple dependent variables (circRNAs) together

with the two independent variables (Sham,TBI/different timepoints). For The behaviour experiment among different groups with different virus injection (fig. 14,15 and 16), an ordinary one-way analysis of variance (ANOVA) test was used with post-hoc Tukey correction for multiple comparisons. Western-blot data were analysed by non-parametric Kruskall-Wallis ANOVA with Dunn´s post-hoc multiple comparisons test. A difference at $P < 0.05$ was considered to be statistically significant.

3 Results

3.1 The spatio-temporal expression of circular RNAs in mouse brain

Neuros play an important role in brain repair after injury. Exploring mechanisms underlying neuronal synaptic plasticity and synaptic development is of significance in understanding injury-induced synaptic remodelling. Herein, our study focusses on unveiling the potential role of circRNAs in these processes, because these molecules are known to regulate synapse development in neurons and are relevant to memory deficits following TBI.

First of all, we selected candidates from bio-informatic screenings using GEO DataSets (GSE61991) for synapse-related, circRNAs encoding genes. Among them, over one thousand of these selected genes are synapse-related and can produce thousands of circRNAs, however there are only ten percent of circRNAs that can be conservatively expressed in humans (data generated by circBANK). In order to further explore the special function of circRNA, we analysed the location of selected circRNA in different brain regions and neuronal subcellular compartments with the CIRCpedia website. We selected 25 circRNAs that are highly expressed in the synaptosome as our research objects, and one low-expression circRNA (from the DLG1 gene, labelled DLG1-2) as negative controls (Figure 3).

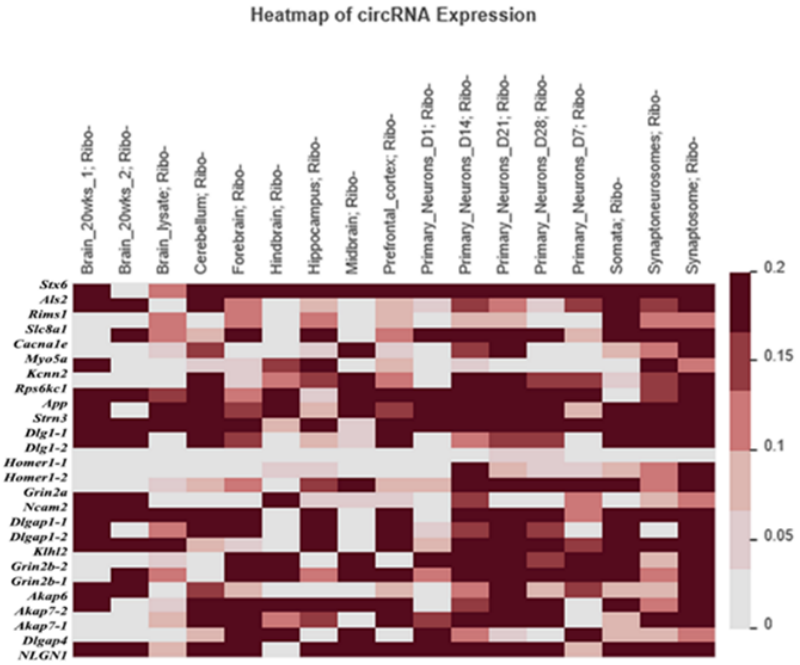

Figure 3. The spatio-temporal expression of circRNA was identified in mouse brain by CIRCpedia analysis. A) The following three criteria of circRNAs are used to select the object of our research: 1. the circRNA produced by the synapse-related genes; 2. the enriched in neuron and synaptosome

analysed by CIRCpedia v2 website; 3. the conserved in human and mouse.

3.2 CircRNA Profiling in mouse hippocampus tissues after TBI

In order to verify the results of our predictions, and to identify changes in circRNAs expression patterns in hippocampus of post-TBI, we performed circRNA analysis using cDNA synthesised from RNA which was isolated from sham or TBI mouse hippocampus at different timepoints. We performed analysis on circRNAs enriched in synaptosome with CIRCpedia v2 website including DLG1-2 (Fig. 3). We measured 26 circRNAs (including one negative control), which are conserved human and mouse from sham or 3h, 3dpi and 7dpi post-TBI (N=8 each). There are 14 up-regulated circRNAs successfully verified in mouse hippocampus by real-time fluorescence quantitative PCR (qRT-PCR) using special (span-junction or back-splicing) primers[132]. Expression analysis showed that compared with the sham group, all these 25 circRNAs, which are encoded by synapse-related genes, showed an increasing trend in the hippocampus after TBI, especially at the 7 days timepoint. This time point is also the peak period of nerve recovery after the mouse traumatic brain injury model. This finding is consistent with predicted results. Subsequently, we found that several of circRNAs were indeed differentially expressed at different timepoints (Fig. 4A). Two-way multivariate ANOVA (MANOVA) revealed significant differences in the time-course ($F=2,059$, Wilks = 0.024, $p=0.011$). The Post hoc analysis (Two-way ANOVA, Tukey corrected) revealed a significant increase of circRNA-1679 (from Klhl2) at 7 days timepoint (Fig. 4B, $F(3, 21)=9.8$ $p=0.0007$ TBI-7d vs. Sham), as well as circRNA-8828 (from ALS2) (Fig. 4C, $F(3, 21)=6.7$ TBI-3d $p=0.0035$ vs. Sham and TBI-3d $p=0.0069$ vs. Sham), circRNA-0153 (from Akap7) (Fig. 4D, $F(3, 21)=8.9$ TBI-3d $p=0.0018$ vs Sham), circRNA-0810 (from Dlgap1) (Fig. 4E, $F(3, 21)=6.8$ TBI-3d $p=0.0137$ vs. Sham and TBI-7d $p=0.0143$ vs. Sham), circRNA-0811 (from Dlgap1) (Fig. 4F, $F(3, 21)=7.4$ TBI-3d $p=0.0457$ vs. Sham and TBI-7d $p=0.0021$ vs. Sham), circRNA-6522 (from Grain2a) (Fig. 4G, $F(3, 21)=5.040$ TBI-7d $p=0.0155$ vs. Sham), circRNA-1530 (from Grain2b) (Fig. 4H, $F(3, 21)=4.316$ TBI-7d $p=0.0196$ vs. Sham), circRNA-7052 (from Slc8a1) (Fig. 4I, $F(3, 21)=14.07$ TBI-3d $p<0.0001$ vs. Sham), circRNA-0491 (from Homer1) (Fig. 4J, $F(3, 21)=6.1$ TBI-7d $p=0.0032$ vs. Sham), circRNA-0705 (from App) (Fig. 4K, $F(3, 21)=8.89$ TBI-7d $p=0.0030$ vs. Sham), circRNA-0132 (from Rps6kc1) (Fig. 4L, $F(3, 21)=4.16$ TBI-3h $p=0.0177$ vs.

Sham), circRNA-0372 (from Strn3) (Fig. 4M, F (3, 21)=24.21 TBI-7d p<0.0001 vs. Sham), circRNA-0091 (from Stx6) (Fig. 4N, F (3, 21)=10.65 TBI-3d p=0.0002 vs. Sham and TBI-7d p=0.0016 vs. Sham), circRNA-0679 (from Dlg1) (Fig. 4O, F (3, 21)=4.312 TBI-7d p= 0.0210 vs. Sham). Taken together, these data show that circRNAs, which are coded by synapse-related gene and enriched in synapses, may function as a special set of synaptic plasticity related mediators in the hippocampus.

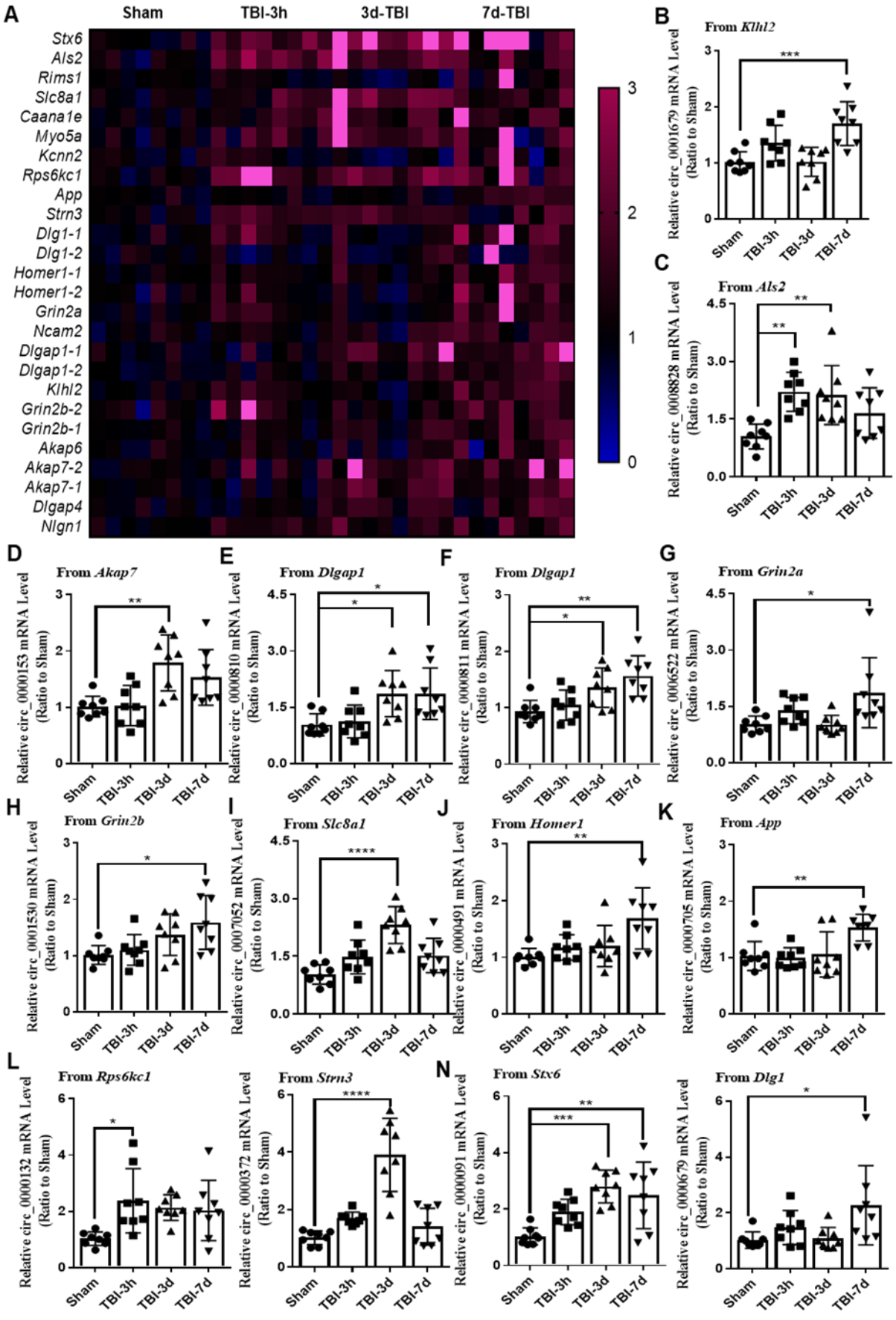

Figure 4. Expression of circRNA in hippocampus of traumatic brain injury at different time points. Expression of 26 circRNAs were screened in the hippocampi of TBI mice at 3h, 3d and 7days. Heatmap of the circRNA mRNA expression at 3h, 3d and 7days after sham or TBI. A) Real−time PCR

analysis of circRNAs showed the significant increase of circRNA-1679 (from klhl2) (B, TBI-7d p=0.0004 vs. sham), circRNA-8828 (from ALS2) (C, TBI-3h p=0.0025 vs. sham and TBI-3d p=0.0053 vs. sham), circRNA-0153 (from Akap7) (D, TBI-7d p=0.0035 vs. sham), circRNA-0810 (from Dlgap1) (E, TBI-3d p=0.0407 vs. sham and TBI-7d p=0.0014 vs. sham), circRNA-0811 (from Dlgap1) (F, TBI-3d p=0.02 vs. sham and TBI-7d p=0.0208 vs. sham), circRNA-6522 (from Grain2a) (G, TBI-7d p=0.0159 vs. sham), circRNA-1530 (from Grain2b) (H, TBI-7d p=0.011 vs. sham), circRNA-7052 (from Slc8a1) (I, TBI-3d p<0.0001 vs. sham), circRNA-0491 (from Homer1) (J, TBI-7d p=0.0032 vs. sham), circRNA-0705 (from App) (K, TBI-7d p=0.0065 vs. sham), circRNA-0132(from Rps6kc1) (L, TBI-3h p=0.0141 vs. sham), circRNA-0372 (from Strn3) (M, TBI-7d p<0.0001 vs. sham), circRNA-0091 (from Stx6) (N, TBI-3d p=0.0002 vs. sham and TBI-7d p=0.0018 vs. sham), circRNA-0679 (from Dlg1) (O, TBI-7d p=0.0233 vs. sham). The leftover circRNAs not shown in histogram showed no difference between sham and TBI groups in any of the timepoints. (Normalized to *Gapdh*, data shown as mean±SD; group size: sham N=8, TBI-3h N=8, TBI-3d N=8, TBI-7d N=8). *: p<0.05; **: p<0.01; ***: p<0.001; ****: p<0.0001.

3.3 The expression of circKlhl2 and circGrin2a in TBI tissues

In order to further study the expression pattern of circular RNAs in trauma, we extracted RNA from the contralateral hippocampal brain tissue of traumatized mice for comparison. It was found that in most cases, compared with the control group, the expression of circRNAs in the bilateral hippocampus of the trauma group was significantly increased, which may be related to the post-traumatic stress response. However, circKlhl2 and circGrin2a were only significantly increased in the traumatic hippocampus (Fig. 5 A, D). Though the liner Klhl2 and Grain2a were also coded by the same pre-mRNA with circKlhl2 and circGrin2a, linear RNA did not give significant changes after trauma (Fig. 5 B, E). In addition, it was found that there is no significant correlation between circular RNA and the linear structure of the RNA (Fig. 5 C, F). Therefore, we can assume that traumatic brain injury only affects the change of circular Klhl2 and Grain2a, but not their normal gene expression. That is to say, the mechanism of circular RNA in trauma is independent from their linear counterparts.

In summary, circular Klhl2 and Grain2a showed significant increase in the ipsilateral hippocampus compared to the sham and the contralateral hippocampus 7 days post TBI. Considering that these two circRNAs may be related to the damage repair of TBI, and traumatic brain injury did not alter the liner Klhl2 and Grain2a gene expression, we

choose circKlhl2 and circGrin2a as our primary research objects.

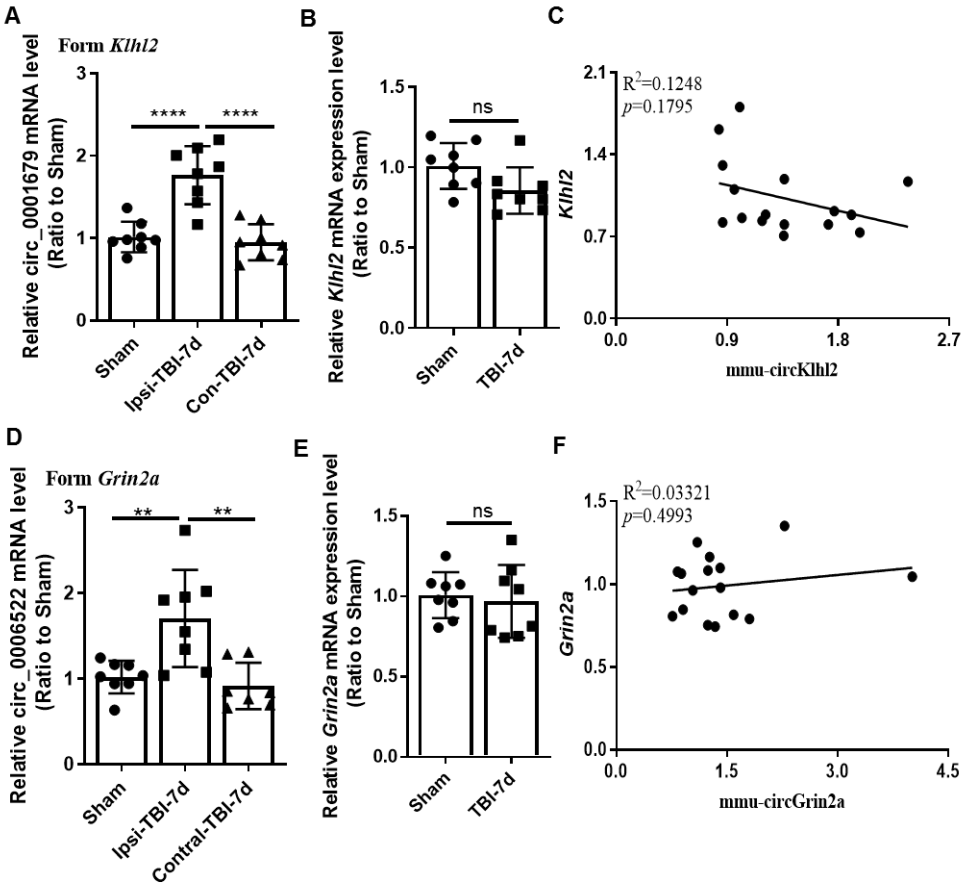

Figure 5. TBI upregulates circKlhl2 and circGrin2a expression but not liner RNA in mouse hippocampus. CircKlhl2 and circGrin2a mRNA level was assessed in the contralateral and ipsilateral sides of 7 days post TBI. A) The expression of circKlhl2 in the ipsilateral side showed significant up-regulation compared with Sham and contralateral sides. B) the liner RNA of Klhl2 did not show significant difference, either. C) Correlation analysis revealed no significant inverse correlation between circKlhl2 and liner Klhl2 in the TBI group (R^2 = 0.1248; p =0.1795). D) The expression of circGrain2a in the ipsilateral side showed significant up-regulation compared with Sham and contralateral sides. E) the liner RNA of Grain2a did not show significant difference, either. F) Correlation analysis revealed no significant inverse correlation between circGrain2a and liner Grain2a in the TBI group (R2 = 0.03321; p =0.4993). (Normalized to *Gapdh*, data shown as mean±SD; data shown as mean±SD; Correlation with linear regression is shown; group size: sham N=8, TBI-3h N=8, TBI-3d N=8, TBI-7d N=8). ns: p>0.05; **: p<0.01; ***: p<0.001; ****: p<0.0001.

In order to further investigate the role of circKlhl2 and circGrin2a in TBI, we collected surgical specimens of human brain samples from Kaifeng Central Hospital from October 2018 and July 2019. These included specimens with different degrees of TBI and controls (such as cerebral haemorrhage or aneurysm surgery fistula). The results showed that circKlhl2 was significantly up-regulated in traumatic brain tissues, which was consistent with the mouse model (Fig. 6 A). However, circGrin2a was significantly down-regulated in traumatic brain tissues of patients, which was contrary to the results

in the mouse model (Fig. 6 D). Consistent with our mouse results, we also did not observe significance of liner Klhl2 and Grin2a and there was no significant correlation between circular RNA and the linear structure of the RNA in human samples (Fig. 6 B, C, E, F). Both show great prospect, however no suitable mouse model was found to further study the changes of circGrin2a, we thus chose circKlhl2 as our main research object.

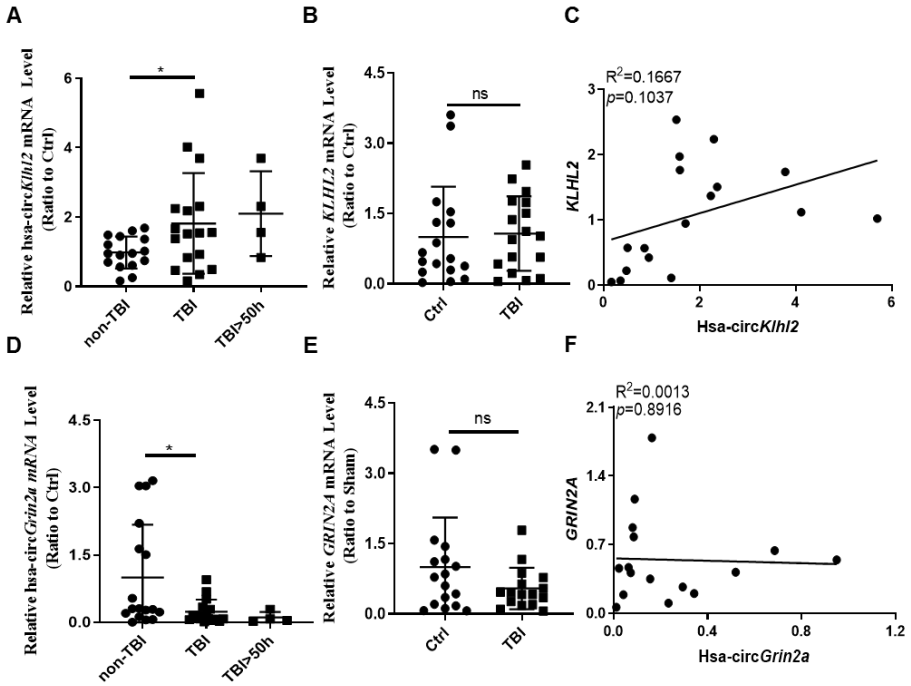

Figure 6. TBI upregulates circKlhl2 and circGrin2a expression in human patients. CircKlhl2 and circGrin2a mRNA level were assessed in human TBI patients. A) The expression of circKlhl2 in TBI patients' surgical specimens showed significant upregulate compared with non-TBI group especially > 50h after TBI. B) the liner RNA of Klhl2 did not show significant difference. C) Correlation analysis revealed no significant correlation between has-circKlhl2 and liner Klhl2 in the TBI group (R^2 = 0.1667; p=0.1037). D) The expression of circGrin2a in TBI patients' surgical specimens showed significant downregulation compared with non-TBI group. B) the liner RNA of Grin2a did not show significant difference. C) Correlation analysis revealed no significant correlation between has-circGrin2a and liner Grin2a in the TBI group (R^2 = 0.0013; p =0.8916). (Normalized to *Gapdh*, data shown as mean±SD; Correlation with linear regression is shown; group size: non-TBI N=16, TBI N=17, TBI > 50h N=4,). ns: p>0.05; *: p<0.05.

3.4 The basic information of circKlhl2

CircKlhl2 is encoded by exons 3, 4 and 5 of the klhl2 gene, which can be stably expressed after RNase R treatment (Fig. 7 A, B), and no PCR product is produced when genomic DNA is used as a template (Fig. 7 C). CircKlhl2 cannot be degraded by Rnase R, which is known to cleave and degrade RNA from the 3'-5' direction, and digest almost all linear RNA molecules, but not circular RNA [15]. These results show that circKlhl2 is a stable head-to-head structure and can be stably expressed as a circular RNA in mouse

hippocampus. We used the circBANK database to compare the human and mouse

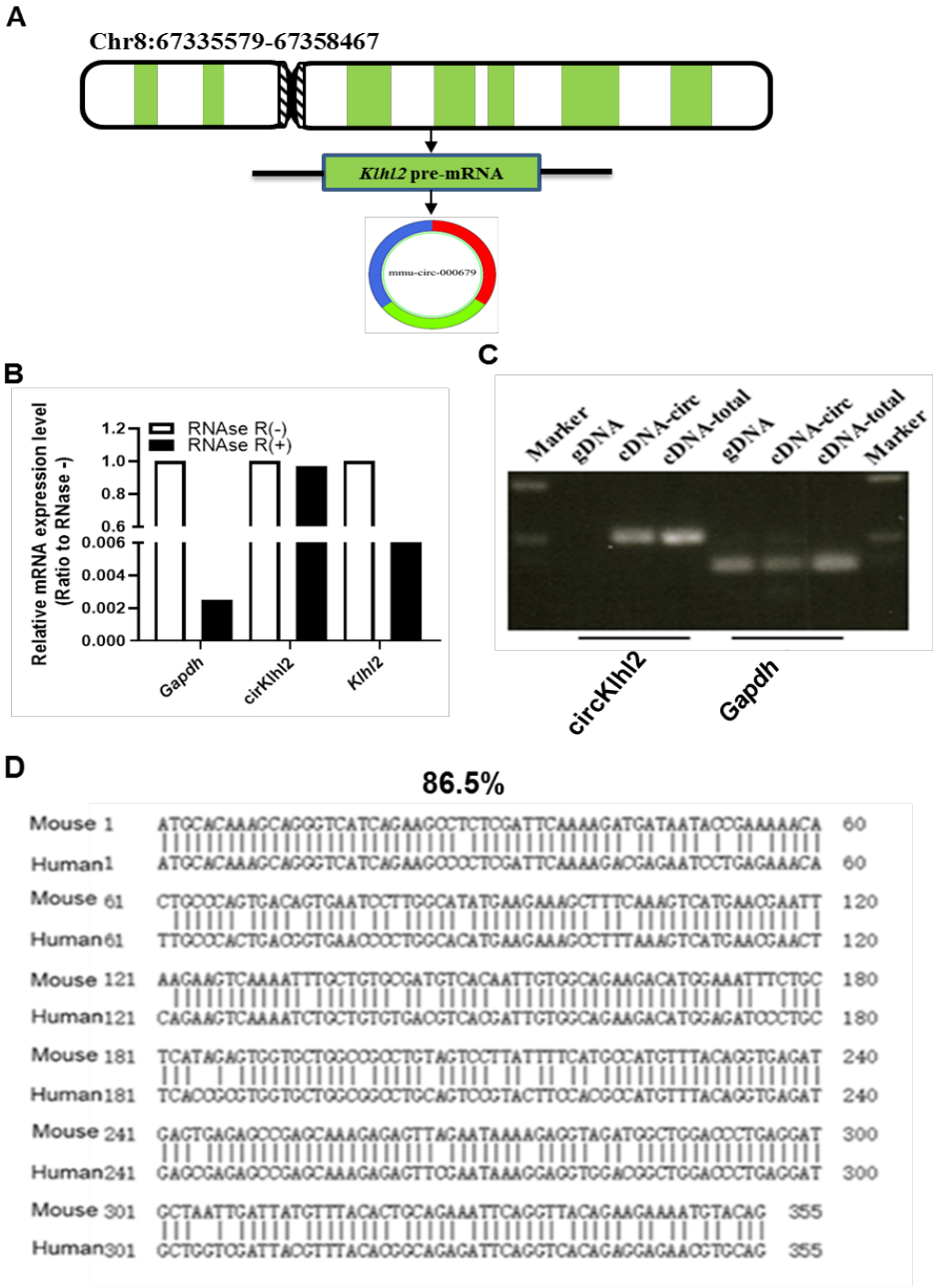

sequences of circKlhl2, and found that these two sequences have 86.5% similarity.

Figure 7. The basic information of circKlhl2. A) Genomic loci of circRNA-00001679 gene. circRNA-00001679 (circKlhl2) is produced at the Klhl2 gene locus from circBase. B) CircKlhl2 cannot be degraded by RNase R. C) Divergent primers amplified circKlhl2 from cDNA, but not genomic DNA (gDNA). D) Pairwise alignment of the human and murine circKlhl2 sequence show 86.5% homology.

In order to study the basic localization and function of circKlhl2, we used BaseScope to perform in situ hybridization followed by co-localization staining with the markers of neuron (MAP 2), astrocytes (GFAP) and microglia (IBA1), three main types of cells in the central nervous system. The results showed that circKlhl2 was expressed in all three types of cells, but was mainly distributed in the cell body of neurons, shown by co-

staining with MAP2 (Figure 8 A). At the same time, we tested the motor neurons in the mouse spinal cord. The results are similar to the expression in the hippocampus.

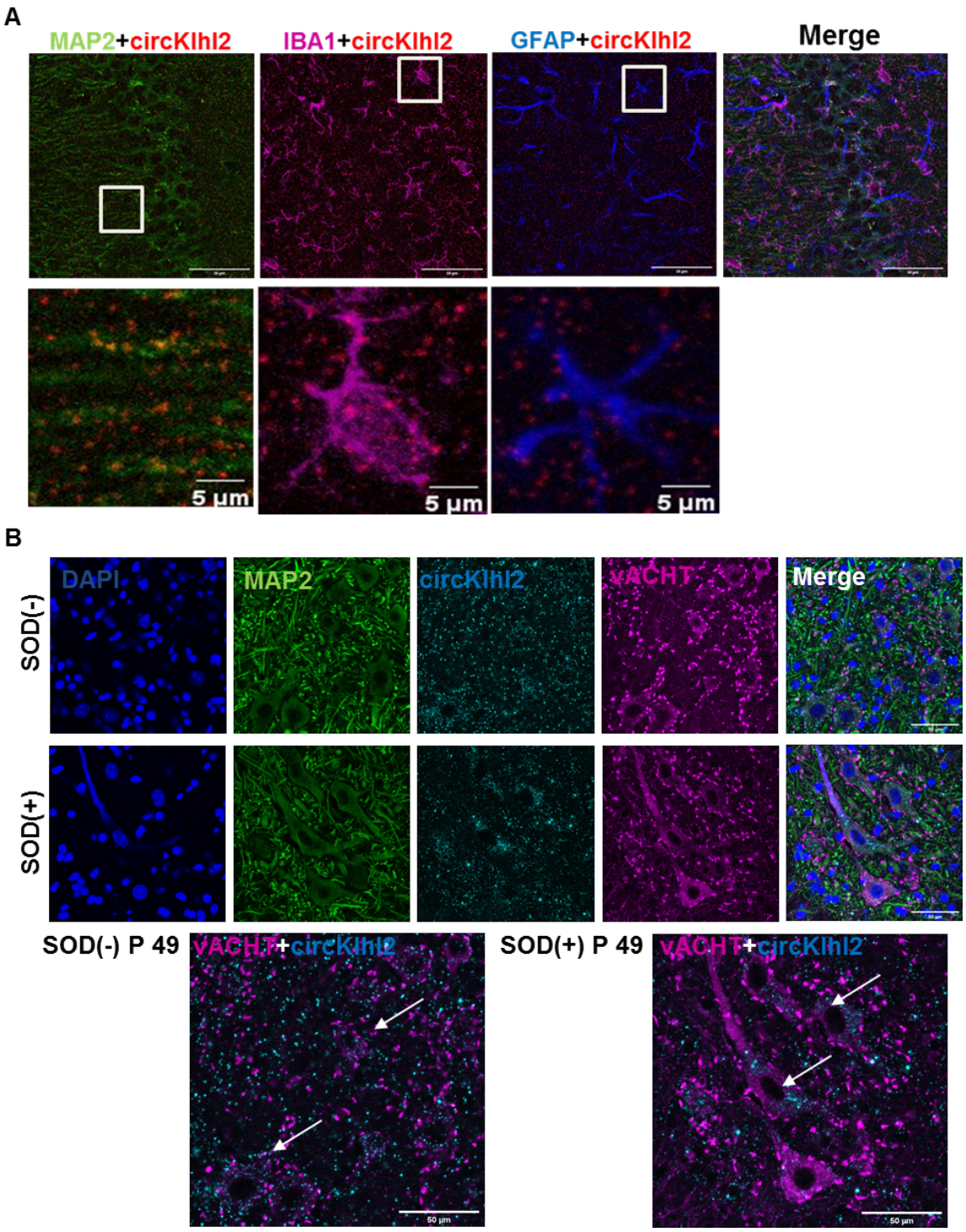

Figure 8. circKlhl2 were enriched in neurons. A) Single mRNA molecule In Situ Hybridization for circKlhl2 mRNA co-stained with GFAP, IBA1 and MAP2 in hippocampus. The number of circKlhl2 mRNA molecules was visualized more in the Map2 positive cells (neuron) vs IBA1 (microglia) and GFAP (astrocytes) positive cells. B) Single mRNA molecule In Situ Hybridization for circKlhl2 mRNA co-stained with DAPI, vACHT and MAP2 in spinal cord. The number of circKlhl2 mRNA molecules was visualized abundantly in the vACHT positive cells and showed decreased expression in SOD (+) compared with SOD (-) mice. Magnification 40X, scale bars = 50 micrometers (µm).

CircKlhl2 is also highly expressed in neurons, especially motor neurons. More interestingly, in the case of SOD gene mutations in ALS, the expression pattern and the amount of circKlhl2 showed significantly changes, but the specific mechanism needs further investigation.

3.5 The expression level of circKlhl2 in different regions of hippocampus.

In order to understand the expression patterns of circKlhl2 in the hippocampus post TBI, we selected the hippocampal regions DG, CA1, CA2 and CA3 and analysed the amount of circKlhl2 in each of these areas 7 days after injury. We found that in the DG, CA1 and CA2 regions, circKlhl2 expression was significantly upregulated (Fig.9 A, B, C, D; Fig.10 A, E), while CA3 displayed an increasing trend but without significant difference (Fig.10 B, F). In another nerve injury model, the optic nerve injury, we have seen a similar expression profile of circKlhl2 in neurons post injury. Despite this, the mechanism for circKlhl2 involvement in TBI and optic nerve damage remains unclear.

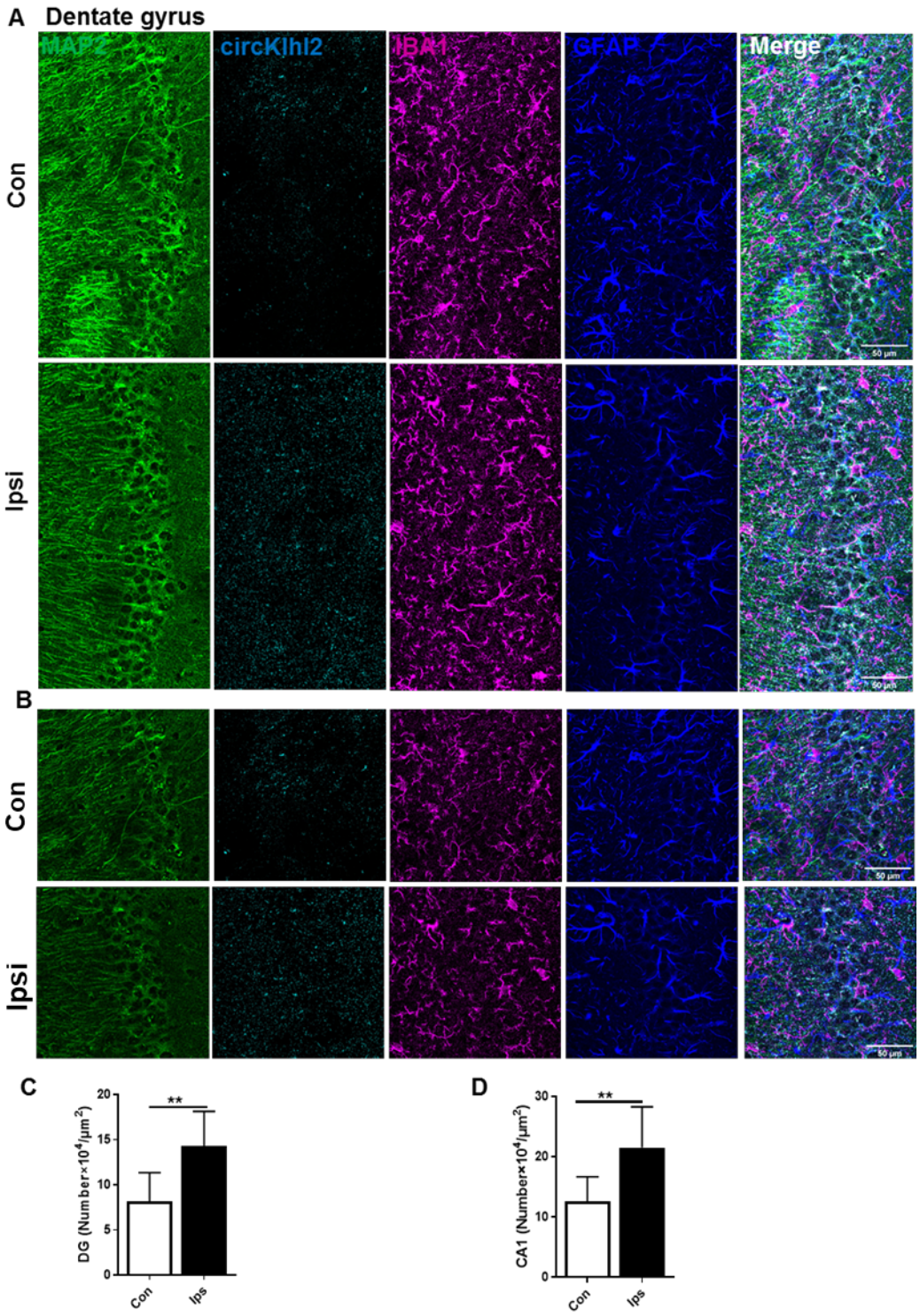

Figure 9. The expression of circKlhl2 in DG and CA1 of hippocampus. Single mRNA molecule In Situ Hybridization for circKlhl2 mRNA co-stained with MAP2 (green) IBA1 (magenta) and GFAP (Blue) in mice 7 days post TBI.A-C) The number of circKlhl2 mRNA molecules was significantly increased in ipsilateral side vs. contralateral side; B-D) Analysis of circKlhl2 in CA1 region showed the significant increase compared with contralateral side; Magnification 40×, scale bars=50 μm. (data shown as mean±SD; group size: TBI-7days N=4,); **: $p<0.01$; two-side unpaired students t-test.

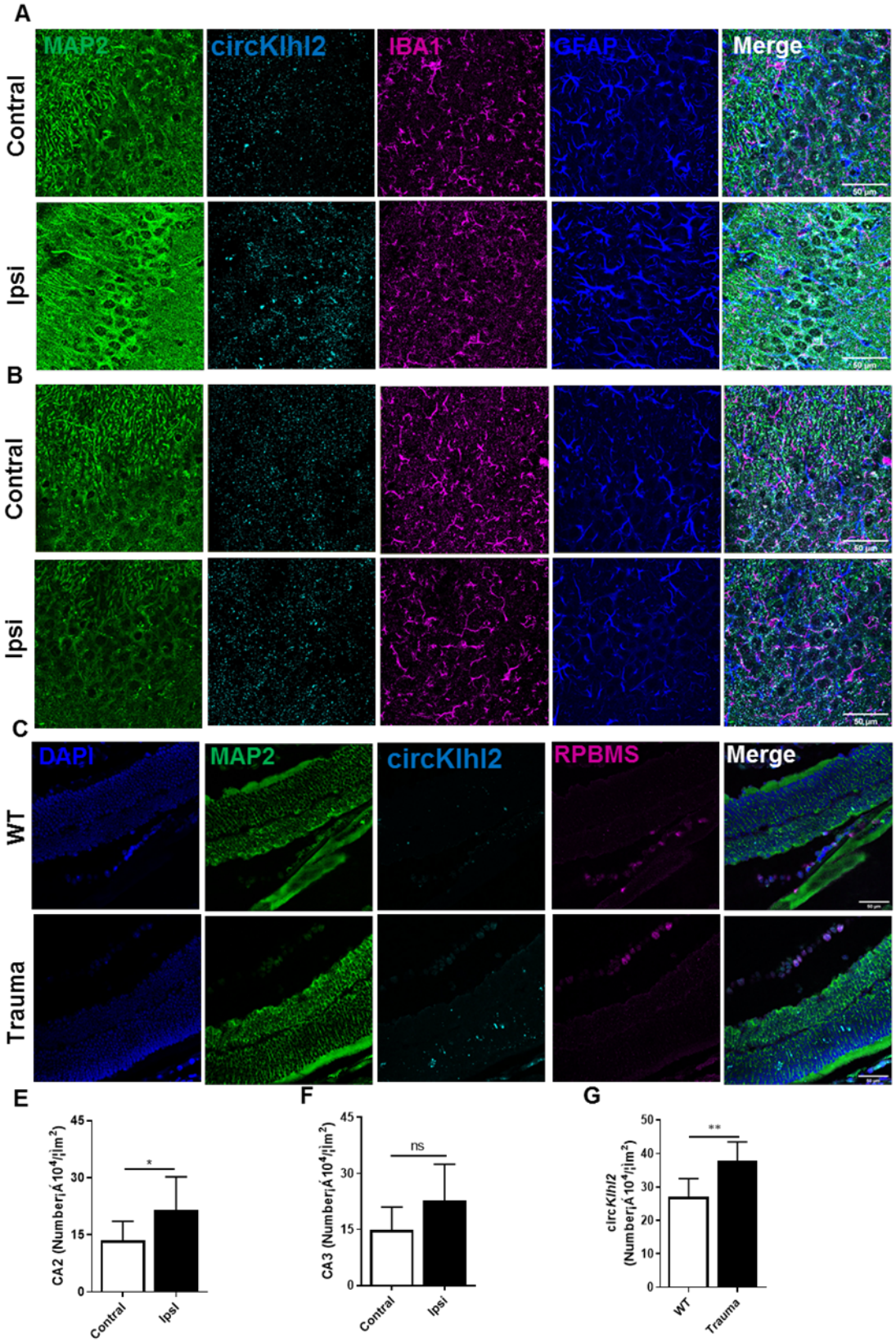

Figure 10. The expression of circKlhl2 in CA2 and CA3 of hippocampus and optic nerve. A-C). The number of circKlhl2 mRNA molecules was significantly increased in ipsilateral side vs. contralateral side; B) Analysis of circKlhl2 in CA1 region showed the significant increase compared with contralateral side; Magnification 40×, scale bars=50 µm. (Data shown as mean±SD; group size: TBI-7days N=4, optic-sham N=4, post-crushed 3days N=5) ns: $p>0.05$, *: $p<0.05$; **: $p<0.01$; two-side unpaired students t-test.

3.6 Generation of circKlhl2 interference and overexpression plasmids

To understand the role of circKlhl2 in the hippocampus after TBI, we generated circKlhl2 interference and overexpression plasmids that were transiently co-transfected into Neuro-2a cells (N2A). For the knock down experiment, we used the span-junction sequence to guarantee the specificity of siRNA and constructed the interference plasmid with the same sequence (Fig.11 A). We detected the interference efficiency exceeded 70% but the linear RNA was not altered, as demonstrated by qRT-PCR (Fig.11 B, C).

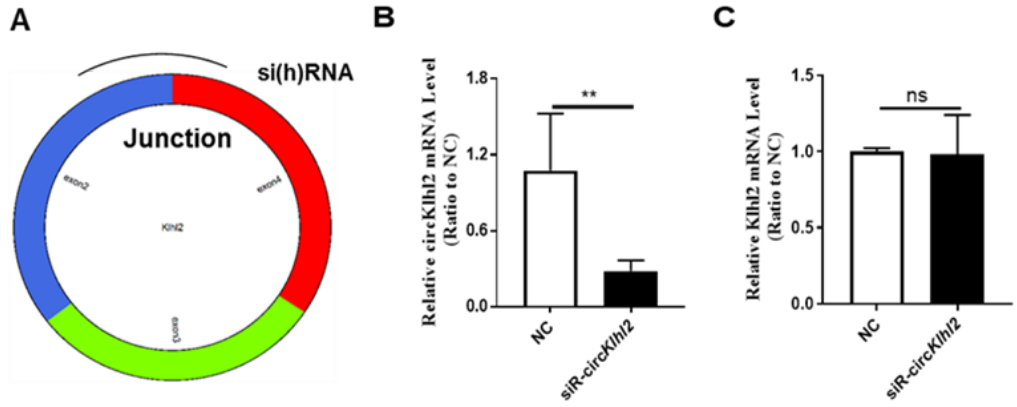

Figure 11. Generation of circKlhl2 interference plasmids. A) the siRNA and shRNA sequence is spanning exon 2 and 4 junctions of circKlhl2. B) Real time-qPCR analysis of endogenous circKlhl2 expression in knockdown plasmid treated mouse N2a cells vs. negative control (control plasmid). C) RT-qPCR analysis of linear Klhl2 mRNA levels in overexpression plasmid-treated N2a cells vs negative control (control plasmid). Normalized to *Gapdh*. Data shown as mean±SD of four independent experiments/group. ns: $p>0.05$, $^{**}p < 0.01$, two-side unpaired students t-test.

In the case of the overexpression of circKlhl2, we designed an overexpression sequence, which could become circular by adding two short "help" sequences to the circKlhl2 exons at the back-splicing junction. Thereby we could distinguish plasmid-derived circRNA from endogenous circKlhl2 (Fig.12 A). QRT-PCR confirmed that the plasmids generated contain mature circRNAs (Fig.12 B), with the appropriate splicing junctions, and with increased endogenous circKlhl2 levels (Fig.12 C). Nevertheless, overexpression of circKlhl2 had no effect on the expression of the linear circKlhl2 mRNA (Fig.12 D).

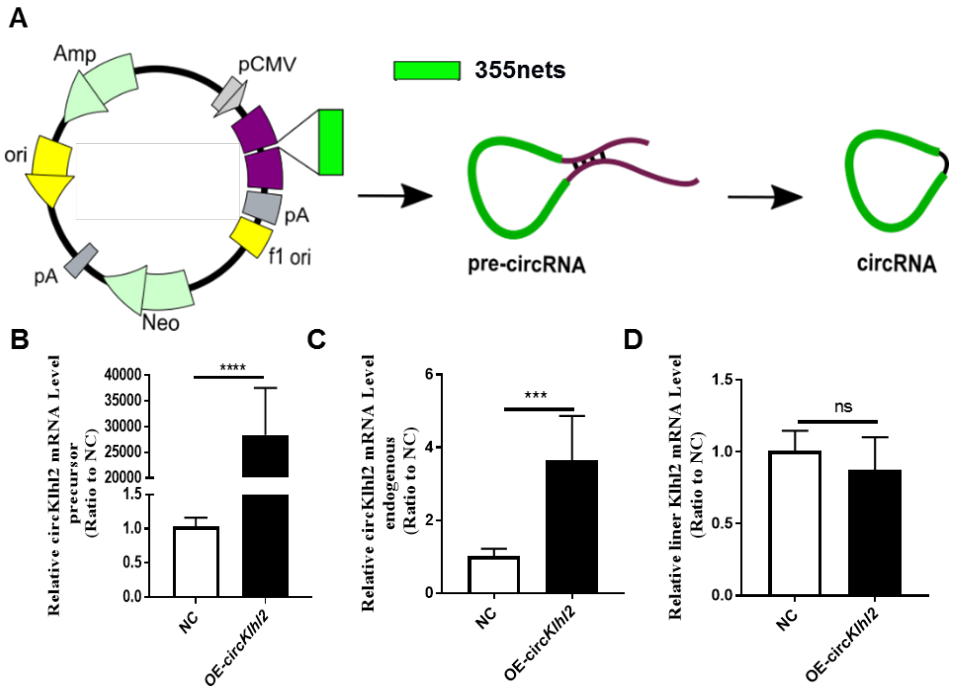

Figure 12. Generation of circKlhl2 overexpression plasmids. A) Exons 2,3 and 4 of the mouse Klhl2 gene were inserted into plasmids, which harbour inverted helper repeat sequences that promote back splicing. B, C) Real time-qPCR analysis of precursor-circKlhl2 and endogenous circKlhl2 expression in control plasmid or circKlhl2 overexpression plasmid-treated mouse N2a cells. D) RT-qPCR analysis of linear Klhl2 mRNA levels in control plasmid or Klhl2 overexpression plasmid-treated N2a cells. Normalized to *Gapdh*. Data are Mean ± SD of four independent experiments/group. ns: $p>0.05$, ***$p < 0.001$, ****$p < 0.0001$; two-sided unpaired students t-test.

3.7 CircKlhl2 may regulate BDNF via miR-30a-5p, miR-30d-5p and miR-34a-5p

Accumulating evidence has indicated that the circRNAs, that are highly expressed in mouse tissues and in human cell lines, act as competing endogenous RNA (ceRNA) sponges, because they can interact with miRNAs and influence the expression of their target proteins. Bioinformatics analysis (RegRNA 2.0) revealed that the binding site of miR-30a-5p, miR-30d-5p, miR-34a-5p and miR-376b-3p were present on circKlhl2 sequence. Previous data show that miR-30a-5p was downregulated after spinal cord injury [34]and chronic mild traumatic brain injury[24]. miR-30d-5p might promote neuronal death by inhibiting autophagy, resulting in delay of neurological recovery and impairment in behavioural performance of rats subjected to Hypoxic–Ischemic Injury[130]. When overexpressing circKlhl2 in the N2a cell line, we found a significant downregulation of miR-30a-5p and miR-30d-5p compared to the negative control ($p=0.0198$ and $p=0.0393$, respectively). Furthermore, when knocking down circKlhl2 in the N2a cell line, we found a trend towards an increase in miR-30a-5p and miR-30d-5p, although not significant (Fig13. A-D). In addition, miR-34a-5p also showed a similar trend with them after overexpressing plasmid treatment ($p=0.0836$, data not show),

but not reaching significance. These results suggested that when overexpressing circKlhl2, it may act as a sponge of miR-30a-5p and miR-30d-5p and in fact negatively modulates the expression of miR-30a-5p.

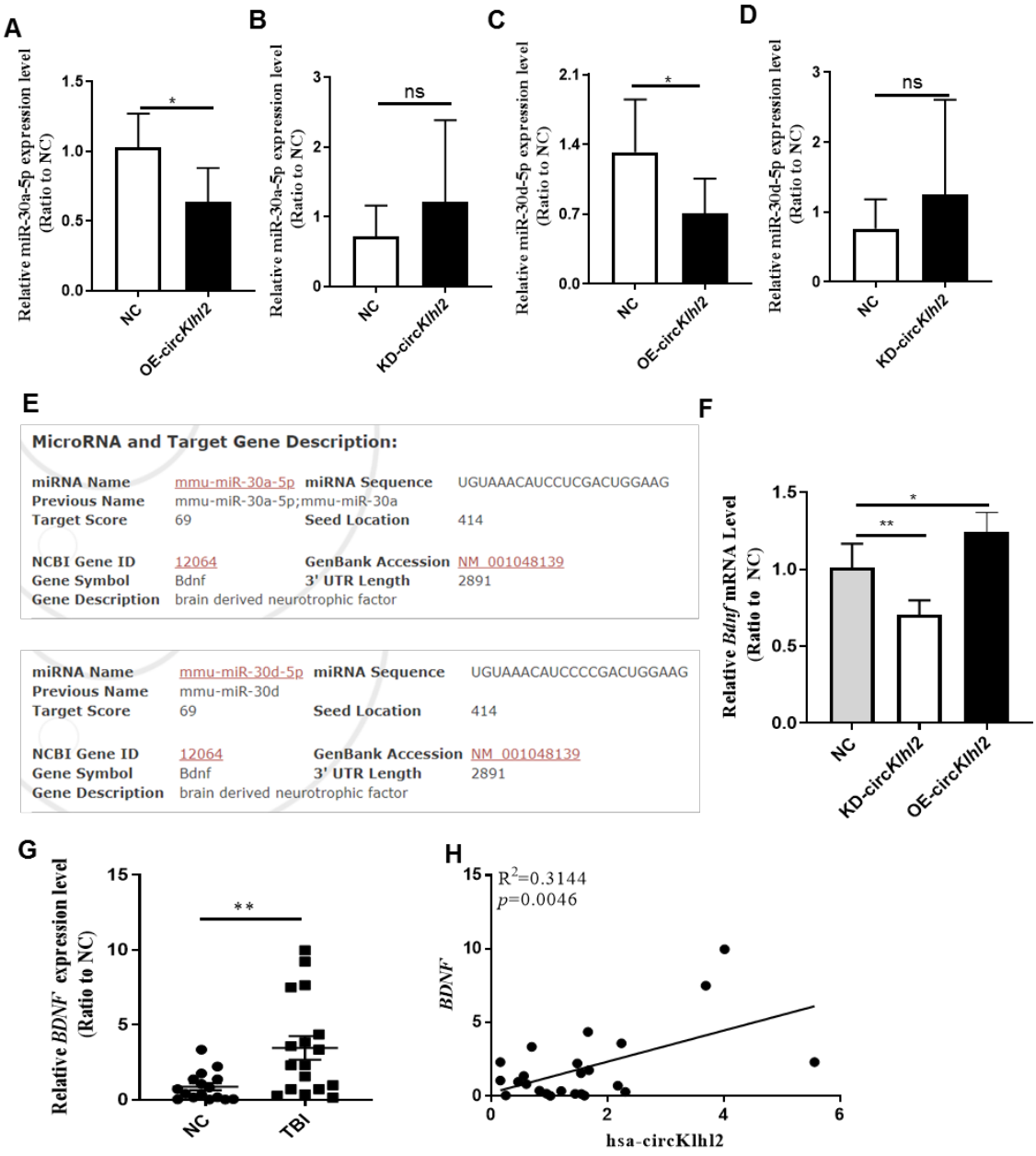

Figure 13. circKlhl2 may serve as a molecular sponge for miR-30a-5p, and miR-30d-5p negatively regulated their expression. A, B, C, D) The relative expression of miR-30a-5p, miR-30d-5p and miR-34a-5p in N2A cell line after circKlhl2 overexpression and interference plasmid transfection. E) miR-30a-5p and miR-30d-5p all potentially target brain-derived neurotrophic factor (BDNF). F) QRT-PCR was used to detect *Bdnf* mRNA expression after overexpression and interference of circKlhl2 in N2A cell line. G) The expression level of *Bdnf* mRNA showed significantly upregulated in human TBI samples compared with negative control without TBI. H) Correlation analysis revealed the significant correlation between has-circKlhl2 and *Bdnf* mRNA expression level in the TBI group (R^2=0.3144; p=0.0046). Normalized to *Gapdh* and U6. Data are Mean ± SD of three independent experiments/group (two-sided unpaired students t-test). (Human patients group size: non-TBI N=16, TBI N=17. Correlation with linear regression is shown;) ns: p>0.05, *p < 0.05, **p < 0.01 vs. negative control or non-TBI,

Using miRNA target prediction algorithms and previously published studies, we found

that miR-30a-5p, miR-30d-5p, and miR-34a-5p (data not shown) all potentially target brain-derived neurotrophic factor (BDNF), which is the most important factor for cell survival during TBI. Interestingly, we also found that BDNF is significantly upregulated in the N2a cell line by overexpressing circKlhl2 (Fig13. F). In fact, when knocking down circKlhl2, we find BDNF was also downregulated (Fig 13. F). Furthermore, when investigating the BDNF expressing in human TBI samples, we detected an upregulation of its expression post-injury, which was also significantly correlated to the expression of circRNA in human samples (Fig13. G, H). Therefore, further work is necessary to investigate more target genes in addition to BDNF to clarify the mechanisms underlying the miR-30a-5p and miR-30d-5p function in TBI.

3.8 Overexpression of circKlhl2 may ameliorate Anxiety-Like Behaviour

To determine whether circKlhl2 interference and overexpression affect the functional outcome post injury, we performed a series of hippocampal specific behavioural tests while overexpressing and knocking down circKlhl2 in TBI. Overexpression and knockdown were done by intracerebral injection of an AAV into the hippocampus 30 days prior to the TBI (Fig.14 A). In the open filed test (OFT), we established six groups of mice, and they were tested under the similar traveling distance. In sham group, we found that the mice received injectionon of AAV- circKlhl2-shRNA spent less time in the central region of the open field compared to WT mice with AAV-NC virus; in the TBI group, we found mice administered with AAV-NC and AAV-circKlhl2-shRNA also spent less time in the central region of the open field compared to WT mice injected with AAV-NC virus, except the mice with AAV-circKlhl2-OE virus spent same time in the central region (Fig.14 B). The above results can only indicate a trend of change due to quantitative reasons, and reveal no significant statistical difference. For the visit times in in the central region of the open field, we only found the number of TBI mice injected with AAV-circKlhl2-shRNA visit less than the other groups. Taken together, these results indicate that circKlhl2 overexpression may reduce anxiety-like behaviour in TBI mice.

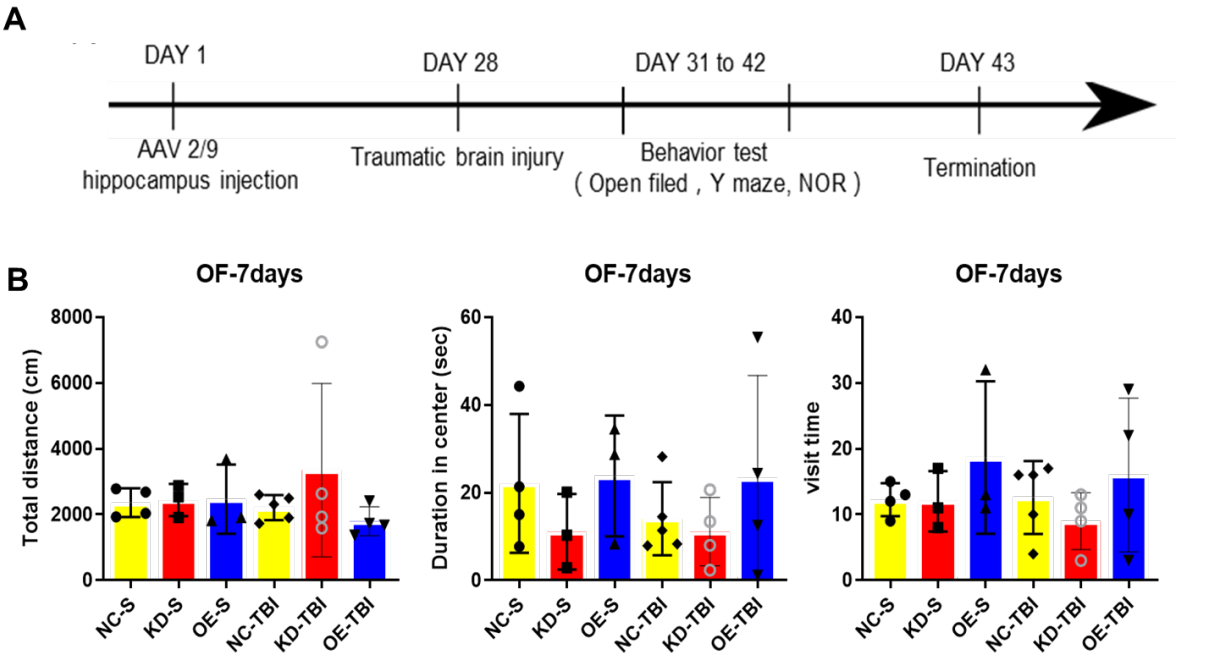

Figure 14. Effects of circKlhl2 interference and overexpression on anxiety-like behavior after TBI. (A) The workflow of our experiments. 5 weeks old, WT mice received different virus (AAV-NC; AAV-circKlhl2-shRNA and AAV- circKlhl2-OE) via hippocampus injection and followed by TBI operation. (B) Total distance, time spent in the center and number of entries into the center, in open field test were quantified and analyzed. (Data are Mean ± SD.; group size: AAV-NC-Sham n=4, AAV-NC-TBI n=5, AAV-circKlhl2-shRNA-Sham n=3, AAV-circKlhl2-shRNA-TBI n=3, AAV-circKlhl2-OE-Sham n=3, AAV-circKlhl2-OE-TBI n=4). *p < 0.05, **p < 0.01, ***p < 0.001 vs. AAV9 control treated mice (One-way ANOVA).

3.9 Overexpression of circKlhl2 enhanced spatial memory

For the Y maze test, we calculated the percentage of spontaneous alternation performance (SAP) (Fig.15 A). The TBI resulted in a significant decrease of SAP compared to the sham at a 7 days timepoint (p=0.0051), and this difference completely disappeared at 14 days, suggesting regeneration of spatial memory after TBI at 14 days. Interestingly, the overexpression of circKlhl2 in TBI resulted in a significant increase of SAP compared to TBI alone at the 7 days timepoint (p=0.0478), with a comparative SAP to the sham group, suggesting a beneficial effect of circKlhl2 on spatial memory post TBI (Fig.15 B).

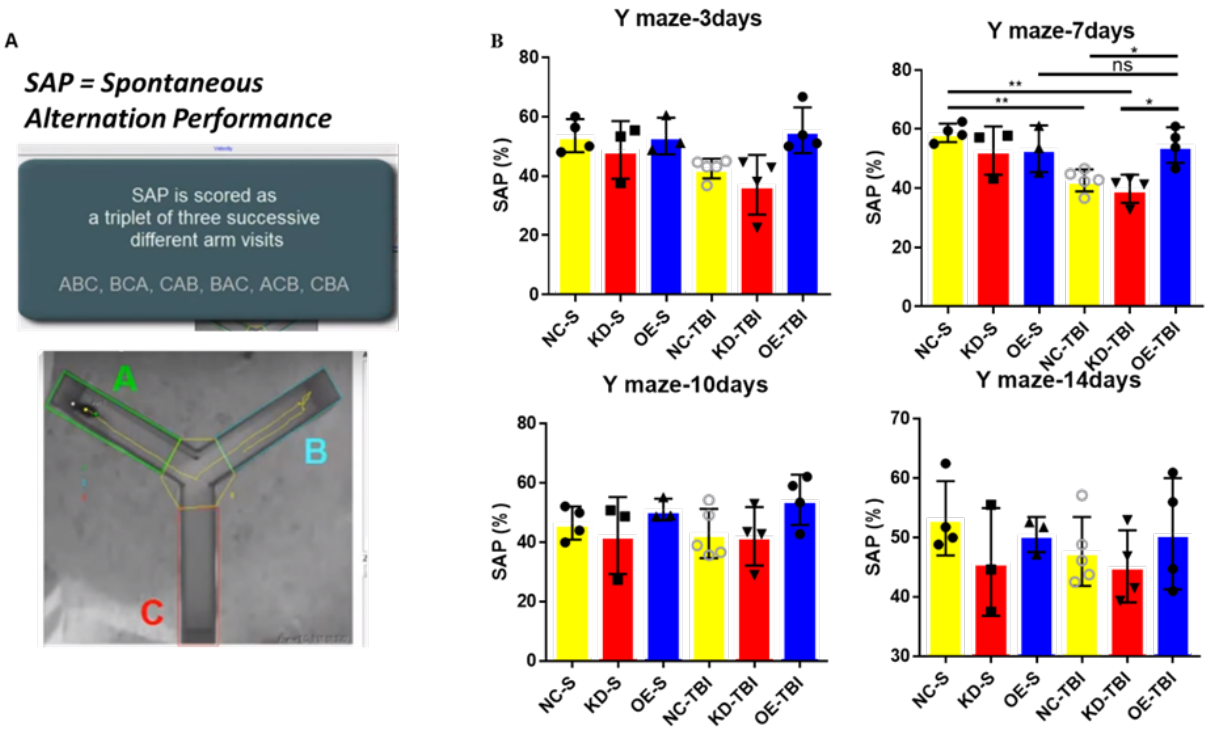

Figure 15. Spontaneous alternation performance after TBI with treatment by negative control, circKlhl2 shRNA or circKlhl2 overexpression AAV treatment. A) SAP is scored as a triplet of three successive different arm visits. B) Traumatic brain injury can significantly decrease percentage of correct alternation compared with sham group at third and seventh day. After the tenth days, the memory of the trauma group gradually recovered, and there was no significant statistical difference when compared with the sham group. AAV9 mediated overexpression of circKlhl2 improved memory recovery but interference of circKlhl2 declined this effect. Compared to AAV-NC-Sham (n =4 mice). (Data are Mean ± SD. Group size AAV-NC-Sham n=4, AAV-NC-TBI n=5, AAV-circKlhl2-shRNA-Sham n=3, AAV-circKlhl2-shRNA-TBI n=3, AAV-circKlhl2-OE-Sham n=3, AAV- circKlhl2-OE-TBI n=4). ns: $p>0.05$, $^{**}p < 0.01$ vs. AAV9 control treated mice (One-way ANOVA).

3.10 Overexpression of circKlhl2 may Enhance short-term learning memory

In the novel object (location) recognition test, we did the open filed test before the NOR test, for habituation of the arena. Training of the mice to the two objects was performed 1h after the habituation, and changing the location was done 1h after the training, followed by changing the object another hour after the location change to investigate short-term memory (Fig.16A). When the location of the object was changed, we found that the control TBI and knockdown TBI groups, investigate the object for less time (discrimination index) compared to the sham groups (less than 50%) at both the 5th and the 14th day, although not significant (Fig. 16 B). Interestingly, we found an increase of discrimination index was higher compared to the control and knockdown TBI groups and reached the sham levels (Fig. 16B) at both timepoints. Unfortunately, this did not reach significance. When the object was changed, we found a general trend in lower investigation time of the new object in the TBI groups, albeit not significant

(Fig. 16 C). Since the novel location has been found to be a more hippocampal sensitive task[6] and the novel object to be more a perirhinal cortex sensitive task [8], these data suggest the hippocampus specific effect of circRNA on learning and memory post-TBI.

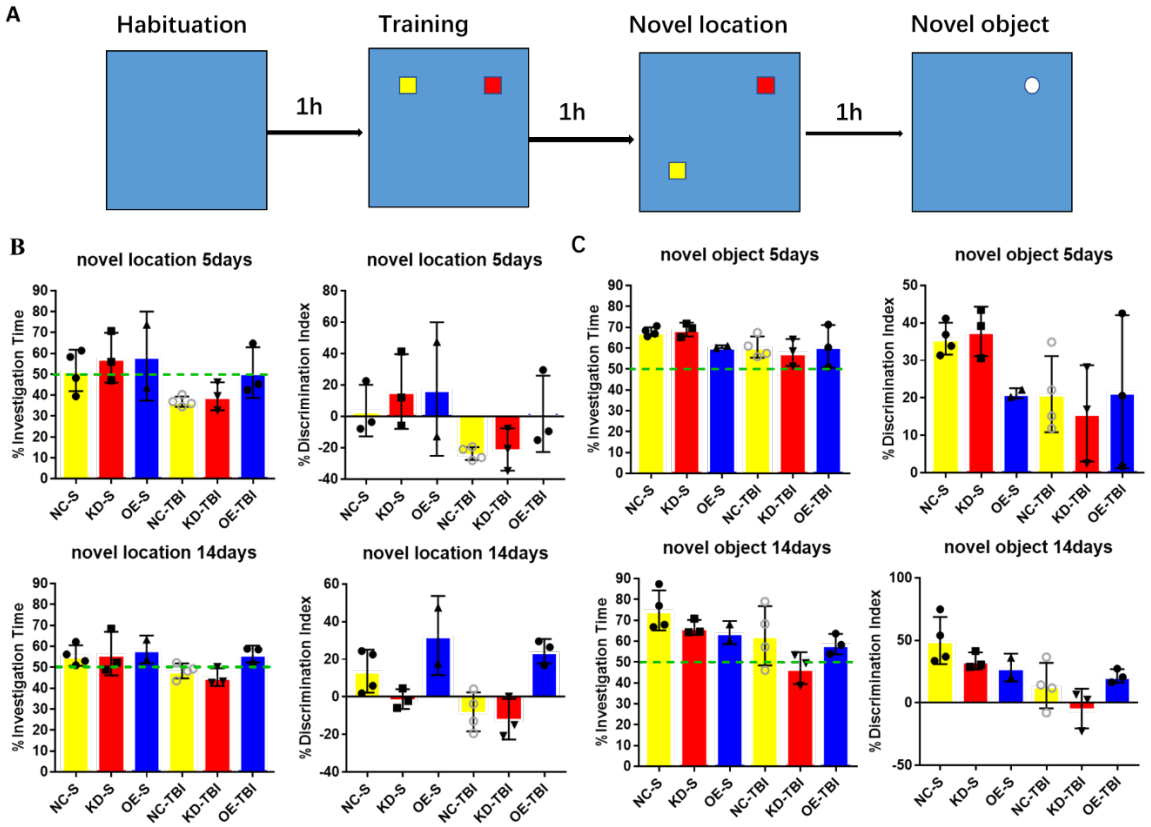

Fig. 16 Novel object recognition after TBI with negative control, circKlhl2 shRNA or circKlhl2 overexpression AAV treatment. A) The workflow of novel (location) object recognition test. B) The investigation time and discrimination index of novel location recognition test on seventh and fourteenth day after TBI.C) the investigation time and discrimination index of novel object recognition test at seventh and fourteenth day after TBI. (AAV-NC-Sham n=4, AAV-NC-TBI n=5, AAV-circKlhl2-shRNA-Sham n=3, AAV-circKlhl2-shRNA-TBI n=3, AAV-circKlhl2-OE-Sham n=3, AAV- circKlhl2-OE-TBI n=4). Data are Mean ± SD. *p < 0.05, **p < 0.01, ***p < 0.001 vs. AAV9 control treated mice (One-way ANOVA).

4 Discussion

Traumatic brain injury (TBI) is the main cause of death and morbidity among young people worldwide. It is reported that there is an incidence of about 300/100.000 or even higher each year. The acute and long-term cognitive and behavioral consequences of TBI (severed, mild and moderate TBI) are very common and often involve hippocampal function, such as memory impairments ranging from acute post-traumatic amnesia to occasional memory impairment or is severe in the case of limited recovery[1, 56]. In fact, in patient's, TBI severely affected the microstructural integrity of the hippocampus[76]. In previous studies, non-coding RNA have been reported in experimental TBI models. It is worth noting that the synaptic circRNAs' function in TBI has not been investigated so far, but enhancing the synaptic plasticity after TBI is known to improve hippocampal function.

CircRNA is an important type of non-coding RNA and has been reported to be involved in CNS diseases, such as glioma, Alzheimer's disease and in brain development, as well as AIS brain injury[69]. However, it has not been investigated in traumatic brain injury (TBI). The present study aimed to detect the altered circRNA expression in the mouse hippocampus after TBI and explore its potential functions. Analyses of the hippocampus in a TBI mouse model and in TBI patients revealed differential expression of several circRNAs, in a similar case for another study utilizing a optic nerve injury model in mice.

CircKlhl2 is conserved and highly expressed in the nervous system, known to be derived from the Klhl2 locus and increased following neuron development[123]. This increase has a substantial impact on the level of synapse-related genes and therefore on synaptic plasticity. Combining in vivo and in vitro studies, we have discovered the regulatory role of circKlhl2 in the process of brain injury and nerve repair. We found that circKlhl2 expression is not associated with its host gene Klhl2 mRNA expression, thus proved that circKlhl2 plays an independent role in the pathophysiology of TBI.

In our study, we found that the level of circKlhl2 was significantly increased in

hippocampus of mouse subjected to TBI and in TBI patients, suggesting that a correlation exists between circKlhl2 and the pathogenesis of brain injury. We must note that our human study was limited by the availability of only cortex and most of the samples were taken within 50 hours after the injury, as patient hippocampus tissue samples could not be used. Universality, conserved expression, defined specificity, high stability, and abundance are the main characteristics of circRNAs that render them very attractive diagnostic tools for assessing diseases[55]. Thus far, circRNAs are potential biomarkers for gastric cancer[51] and hepatocellular carcinoma[80]. A recent study suggested that circRNAs have the potential to be utilized as biomarkers for neurological diseases [58, 63, 129]. Here, the findings of our study regarding the expression and function of circKlhl2 indicate that it has the potential to be a promising biomarker for diagnosing TBI and evaluating the degree of damage caused by traumatic brain injury insults.

We observed that circKlhl2 overexpression can enhance synaptic and cognitive function during a 2-week observation window, post-TBI. Microinjection of shRNA and overexpression circKlhl2 within recombinant adeno-associated virus at 28 d before TBI led to decrease or increase in circKlhl2 expression in respective hippocampus. The mechanism underlying this improvement of outcomes from TBI may be due to enhanced neuronal survival and neuroplasticity via regulating BDNF expression as reported in previous studies[113, 116].

On the basis of bioinformation analysis, we further explored whether synapse-related circRNAs are involved in the synaptic plasticity and neuroprotection in TBI. As we expected, circKlhl2, which was enriched in synapse, may play a key role in the TBI process and recovery. By conducting loss-of-function and gain-of-function experiments, we found that up-regulation of circKlhl2 improved the neurological outcome after TBI and enhanced synaptic plasticity, and these effects were notably abolished by miR-30a/d-5p and miR-34a-5p inhibition.

Computational algorithms such as RegRNA 2.0 have been employed to identify evolutionarily conserved sequences in miR-30a/d-5p and miR-34a-5p that are targeted by circKlhl2. To date, extensive studies have shown that miR-30a/d-5p, which

belongs to the miR-30 family, is expected to target multiple genes related to the genetics or pathophysiology of schizophrenia, including BDNF[70] and NEUROG1[59]. In the case of miR-34a-5p, which can regulates synaptogenesis via coordination of distinct mechanisms in presynaptic and postsynaptic cells[87, 120], only few studies have assessed the role of miR-30a/d-5p and miR-34a-5p in the pathogenesis of traumatic brain injury.

Our study identified that miR-30a-5p and miR-30d-5p and miR-34a-5p levels were negatively regulated by circKlhl2. Overexpression of circKlhl2 significantly downregulated the miR-30a-5p, miR-30d-5p and miR-34a-5p expression in vitro. Although miR-30a-5p is regulated by circKlhl2, our results do not exclude the involvement of other circRNAs or molecules in the regulation of miR-30a-5p, either directly or indirectly. At the same time, we cannot exclude other miRNAs, such as miR-376b-3p, that are reported to be involved in the regulatory process of circKlhl2 in TBI. Therefore, determining whether miRNAs, other than miR-30a/d-5p and miR-34a-5p, bind to circKlhl2 and are involved in neuroprotection and synapse plasticity awaits further investigation.

In previous research and bioinformatics prediction, miR-30a-5p, miR-30d-5p and miR-34a-5p have the same target gene, BDNF, a member of the neurotrophic family of growth factors. BDNF is a key factor in the mechanisms of neuroprotection, synaptic plasticity and the modification of neural networks required for the laying down of memories[32]. Our previous study also indicated that the BDNF plays a critical role in traumatic brain injury [11]. In this study, we identified a new regulatory mechanism of BDNF expression. To our knowledge, this research is the first to demonstrate that BDNF, as a downstream effector of circKlhl2, which is significantly increased in human TBI patient's surgical specimens, lending credence to our speculation that the circKlhl2- miR-30a-5p, miR-30d-5p and miR-34a-5p-BDNF axis contributes to synapse plasticity during TBI.

For the behavioural experiment, we observed that circKlhl2 overexpression significantly reduced cognitive impairment and memory ability caused by TBI especially on the seventh day. Furthermore, it should be noted that other circular RNAs

are also likely to be key players in mediating brain injury and repair, as shown by our data. But we were unable to fully elaborate other mediators, like circGrin2a. In the future, we need to study this using deep sequencing approaches to delineate novel circRNAs and characterize their functional effects.

This conclusion is based on the following experimental findings: (i) circKlhl2 levels are increased 7 days post TBI in mouse hippocampus as well as in cortex tissues from human traumatic brain injury patients; (ii) interference of circKlhl2 can reduce, while overexpression of circKlhl2 can enhance the BDNF expression; (iii) overexpression of circKlhl2 can downregulate the miR-30a-5p and miR-30d-5p expression in vitro; (iv) interference of circKlhl2 significantly decreases and its overexpression tends to increase BDNF expression in vitro;(v) overexpression of circKlhl2 can prevent memory deficits after TBI especially on 7th day ; and (vi) mechanistically, beneficial effects of circKlhl2 appear to mediate cognitive impairment via miR-30a-5p and miR-30d-5p-BDNF signalling axis.

In summary, our data demonstrate that overexpression of circKlhl2 exhibits neuronal protective effects by synaptic plasticity, which preserves post-TBI cognitive function and integrity. We show that this is in part through the miR-30a-5p, miR-30d-5p and miR-34a-5p-BDNF signalling mechanism (Fig. 14). To the best of our knowledge, we show that overexpression of circKlhl2 is a feasible approach to limit traumatic brain injury and may be an attractive option to treat patients with TBI.

5 Summary

Background and purpose: Circular RNAs (circRNA) are a new class of regulatory RNAs originating from end-to-end RNA back-splicing. circRNAs sequester microRNA, bind RNA-binding proteins, epigenetically regulate gene transcription and may even code for small proteins and peptides. The ultimate function of the large number of circRNA remains largely elusive: roles in cell proliferation and stem-cells differentiation have been ascertained. CircRNAs are highly expressed in the brain and initial transcriptome studies have shown that they are modulated in development and by neuronal activity; almost nothing is known about their involvement and function in the brain response to trauma. Nevertheless, circRNAs may be important regulators of microRNAs circuits and may influence acute trauma response and long-term repair. Furthermore, circRNAs are very stable in biological fluids compared to other RNA classes and may constitute a new class of biomarkers, whose potential is largely unexplored.

Methods: We have preliminarily focused on circRNAs derived from synaptic proteins, in order to study their involvement in synaptic remodelling occurring in TBI. We have quantitated the levels of 26 circRNAs from synaptic protein genes in hippocampal samples at 3h, 3d and 7 days after mild TBI. The identification of strongest, significant upregulation of Rps6kc1 at 3h, Stx6 at 3dpi and Klhl2 and Grin2A at 7 dpi, highlight their possible involvement of these transcripts in acute, subacute and reparative response, respectively. Importantly, all these circRNAs have highly conserved homologues in the human transcriptome (as reported in the GEO database). The expression levels of each of these circRNAs were not correlated with the levels of the corresponding protein-coding mRNA, implying that the regulation of circRNAs reflect independent and specific processes. The upregulation of circKlhl2 and circGrin2A (at 7 dpi) is selective for the ipsilateral hippocampus (subject to trauma), compared to the contralateral hippocampus. We established the detection of single-molecule circRNA in situ using the Basescope and confirmed the 1.5 folds elevation of circKlhl2 in the neuronal soma and dendrites of Dentate Gyrus and CA1 (7 dpi) after mild TBI, determining the its neuronal expression. We are collaborating with the Kaifeng Hospital (Kaifeng, China) to determine circRNAs expression in cortical samples

resected from contusive TBI brain lesions (surgery performed 1-100h after trauma) or, as control, during elective neurosurgery. We have been able to confirm the elevation of circKlhl2 in human TBI. The special mechanism of circKlhl2 in TBI was explored by the following means: firstly, we established the circKlhl2 shRNA and overexpression recombinant adeno-associated viruses; secondly, we infected in right hippocampus with AAV2/9-circKlhl2-NC/shRNA/OE viral vectors expressing affected endogenous circKlhl2 expression; thirdly, we did the TBI operation after 28 days after AAV injection, followed by 2 weeks Behavioral Experiment, including open filed, Y maze and novel object/location recognition to measure the anxiety-like behavior, spatial memory and short-term learning memory which is related to hippocampus function and synaptic plasticity.

Results: CircRNAs are important regulators of the acute response to TBI and of the repair mechanism at synaptic level. (i) circKlhl2 levels are increased in post-7days TBI mouse hippocampus as well as in cortex tissues from human traumatic brain injury patients; (ii) interference of circKlhl2 can reduce, and overexpression of circKlhl2 can enhance, the BDNF expression; (iii) overexpression of circKlhl2 can downregulate the miR-30a-5p and miR-30d-5p expression in vitro; (iv) interference of circKlhl2 significantly decreases while overexpression tends to increase BDNF expression in vitro;(v) overexpression of circKlhl2 can prevent memory deficits after TBI especially on 7th day ; and (vi) mechanistically, beneficial effects of circKlhl2 appear to be mediate cognitive impairment via miR-30a-5p, miR-30d-5p and miR-34a-5p-BDNF signalling axis.

Conclusion: Recombinant adeno-associated virus 2/9 circKlhl2 therapy increases circKlhl2 levels in the post-TBI hippocampus leading to its interaction with miR-30a-5p and miR-30d-5p expression in vitro, in turn influences BDNF signalling. This enhances synapse plasticity and preserves post-TBI cognitive mediated function and brain repair.

6 Reference

1. A, A.C., J.W. B, and V.G. C, *Traumatic Brain Injury: An Overview of Epidemiology, Pathophysiology, and Medical Management - ScienceDirect.* Medical Clinics of North America, 2020. **104**(2): p. 213-238.

2. Agoston, D.V., A. Shutes-David, and E.R. Peskind, *Biofluid biomarkers of traumatic brain injury.* Brain Injury, 2017. **31**(9): p. 1195-1203.

3. Ahmed, F., et al., *Time-dependent changes of protein biomarker levels in the cerebrospinal fluid after blast traumatic brain injury.* Electrophoresis, 2012. **33**(24): p. 3705-3711.

4. Bai, Y., et al., *Circular RNA DLGAP4 ameliorates ischemic stroke outcomes by targeting miR-143 to regulate endothelial-mesenchymal transition associated with blood-brain barrier integrity.* Journal of Neuroscience the Official Journal of the Society for Neuroscience, 2017.

5. Baratz, R., et al., *Transiently lowering tumor necrosis factor-α synthesis ameliorates neuronal cell loss and cognitive impairments induced by minimal traumatic brain injury in mice.* J Neuroinflammation, 2015. **12**: p. 45.

6. Barker, G.R. and E.C. Warburton, *When is the hippocampus involved in recognition memory?* Journal of Neuroscience, 2011. **31**(29): p. 10721-10731.

7. Biagas, K.V., et al., *Assessment of posttraumatic polymorphonuclear leukocyte accumulation in rat brain using tissue myeloperoxidase assay and vinblastine treatment.* J Neurotrauma, 1992. **9**(4): p. 363-71.

8. Brivio, P., et al., *Acute stress induces cognitive improvement in the novel object recognition task by transiently modulating bdnf in the prefrontal cortex of male rats.* Cellular and molecular neurobiology, 2020: p. 1-11.

9. Byrnes, K.R., D.J. Loane, and A.I. Faden, *Metabotropic glutamate receptors as targets for multipotential treatment of neurological disorders.* Neurotherapeutics, 2009. **6**(1): p. 94-107.

10.Byrnes, K.R., et al., *Delayed mGluR5 activation limits neuroinflammation and neurodegeneration after traumatic brain injury.* Journal of Neuroinflammation,9,1(2012-02-28), 2012. **9**(1): p. 43-43.

11.Chandrasekar, A., et al., *Neuroprotective effect of acute ethanol intoxication in TBI is*

associated to the hierarchical modulation of early transcriptional responses. Experimental neurology, 2018. **302**: p. 34-45.

12.Chandrasekar, A., et al., *Acute ethanol administration results in a protective cytokine and neuroinflammatory profile in traumatic brain injury.* Int Immunopharmacol, 2017. **51**: p. 66-75.

13.Chen, T., et al., *Down-regulation of Homer1b/c attenuates glutamate-mediated excitotoxicity through endoplasmic reticulum and mitochondria pathways in rat cortical neurons.* Free Radic Biol Med, 2012. **52**(1): p. 208-17.

14.Chen, Z., et al., *Significant changes in circular RNA in the mouse cerebral cortex around an injury site after traumatic brain injury.* Exp Neurol, 2019. **313**: p. 37-48.

15.Cheng, Z.-F. and M.P. Deutscher, *Purification and characterization of the Escherichia coli exoribonuclease RNase R: comparison with RNase II.* Journal of Biological Chemistry, 2002. **277**(24): p. 21624-21629.

16.Chodobski, A., B.J. Zink, and J. Szmydynger-Chodobska, *Blood-brain barrier pathophysiology in traumatic brain injury.* Translational Stroke Research, 2011. **2**(4): p. 492-516.

17.Cogswell, J.P., et al., *Identification of miRNA changes in Alzheimer's disease brain and CSF yields putative biomarkers and insights into disease pathways.* Journal of Alzheimer's disease, 2008. **14**(1): p. 27-41.

18.Commisso, B., et al., *Stage-dependent remodeling of projections to motor cortex in ALS mouse model revealed by a new variant retrograde-AAV9.* 2018. **7**.

19.Cui, X., et al., *hsa_circRNA_103636: potential novel diagnostic and therapeutic biomarker in Major depressive disorder.* Biomark Med, 2016. **10**(9): p. 943-52.

20.Das, D., A. Das, and A. Panda, *Emerging role of long noncoding RNAs and circular RNAs in pancreatic β cells.* Non-coding RNA Investigation, 2018. **2**: p. 69-69.

21.De Bock, M., et al., *The dual face of connexin-based astroglial Ca2+ communication: a key player in brain physiology and a prime target in pathology.* Biochimica et Biophysica Acta (BBA)-Molecular Cell Research, 2014. **1843**(10): p. 2211-2232.

22.Della-Pace, I.D., et al., *Modulation of Na(+)/K(+)- ATPase activity by triterpene 3β, 6β, 16β-trihidroxilup-20 (29)-ene (TTHL) limits the long-term secondary degeneration after traumatic brain injury in mice.* Eur J Pharmacol, 2019. **854**: p. 387-397.

23.Deshpande, L.S., et al., *Alterations in neuronal calcium levels are associated with cognitive deficits after traumatic brain injury.* Neurosci Lett, 2008. **441**(1): p. 115-9.

24.Di Pietro, V., et al., *Salivary MicroRNAs: Diagnostic Markers of Mild Traumatic Brain Injury in Contact-Sport.* Frontiers in Molecular Neuroscience, 2018. **11**(290).

25.Di Pino, G., et al., *Modulation of brain plasticity in stroke: a novel model for neurorehabilitation.* Nature Reviews Neurology, 2014. **10**(10): p. 597.

26.Donkor, E.S., *Stroke in the 21(st) Century: A Snapshot of the Burden, Epidemiology, and Quality of Life.* Stroke Res Treat, 2018. **2018**: p. 3238165.

27.Dorsett, C.R., et al., *Glutamate neurotransmission in rodent models of traumatic brain injury.* Journal of Neurotrauma, 2016: p. 263.

28.Dube, U., J.L. Del-Aguila, and Z. Li, *An atlas of cortical circular RNA expression in Alzheimer disease brains demonstrates clinical and pathological associations.* 2019. **22**(11): p. 1903-1912.

29.Eastman, C.L., R. D'Ambrosio, and T. Ganesh, *Modulating neuroinflammation and oxidative stress to prevent epilepsy and improve outcomes after traumatic brain injury.* Neuropharmacology, 2019: p. 107907.

30.Eliasson, M.J., et al., *Neuronal nitric oxide synthase activation and peroxynitrite formation in ischemic stroke linked to neural damage.* Journal of Neuroscience, 1999. **19**(14): p. 5910-5918.

31.Errichelli, L., et al., *FUS affects circular RNA expression in murine embryonic stem cell-derived motor neurons.* Nature communications, 2017. **8**(1): p. 1-11.

32.Failla, M.D., Y.P. Conley, and A.K. Wagner, *Brain-Derived Neurotrophic Factor (BDNF) in traumatic brain injury–related mortality: interrelationships between genetics and acute systemic and central nervous system BDNF profiles.* Neurorehabilitation and neural repair, 2016. **30**(1): p. 83-93.

33.Fanale, D., et al., *Circular RNA in exosomes.* Circular RNAs, 2018: p. 109-117.

34.Fu, X., et al., *MiR-30a-5p ameliorates spinal cord injury-induced inflammatory responses and oxidative stress by targeting Neurod 1 through MAPK/ERK signalling.* 2018. **45**(1): p. 68-74.

35.Fu, Y., et al., *Circular RNA ABCB10 promotes hepatocellular carcinoma progression by increasing HMG20A expression by sponging miR-670-3p.* Cancer Cell Int, 2019. **19**: p. 338.

36.Ge, X.T., et al., *miR-21 improves the neurological outcome after traumatic brain injury in rats.* Sci Rep, 2014. **4**: p. 6718.

37.Giorgi, C., et al., *Mitochondrial Ca(2+) and apoptosis.* Cell Calcium, 2012. **52**(1): p. 36-43.

38.Giulian, D., et al., *The role of mononuclear phagocytes in wound healing after traumatic injury to adult mammalian brain.* J Neurosci, 1989. **9**(12): p. 4416-29.

39.Goforth, P.B., E.F. Ellis, and L.S. Satin, *Mechanical Injury Modulates AMPA Receptor Kinetics via an NMDA Receptor–Dependent Pathway.* Journal of neurotrauma, 2004. **21**(6): p. 719-732.

40.Gorelick, P.B., *Stroke prevention therapy beyond antithrombotics: unifying mechanisms in ischemic stroke pathogenesis and implications for therapy: an invited review.* Stroke, 2002. **33**(3): p. 862-875.

41.Gourin, C.G. and S.R. Shackford, *Production of tumor necrosis factor-alpha and interleukin-1beta by human cerebral microvascular endothelium after percussive trauma.* Journal of Trauma and Acute Care Surgery, 1997. **42**(6): p. 1101-1107.

42.Guerra, B., et al. *Biogenesis of circular RNAs and their role in cellular and molecular phenotypes of neurological disorders*. in *Seminars in Cell & Developmental Biology*. 2020. Elsevier.

43.Guerriero, R.M., C.C. Giza, and A. Rotenberg, *Glutamate and GABA imbalance following traumatic brain injury.* Current neurology and neuroscience reports, 2015. **15**(5): p. 27-27.

44.Han, B., et al., *Novel insight into circular RNA HECTD1 in astrocyte activation via autophagy by targeting MIR142-TIPARP: implications for cerebral ischemic stroke.* Autophagy, 2018. **14**(7): p. 1164-1184.

45.Hansen, T.B., et al., *Natural RNA circles function as efficient microRNA sponges.* Nature, 2013. **495**(7441): p. 384-388.

46.Henry, R.J., et al., *Inhibition of miR-155 Limits Neuroinflammation and Improves Functional Recovery After Experimental Traumatic Brain Injury in Mice.* Neurotherapeutics, 2019. **16**(1): p. 216-230.

47.Holly, et al., *Clinical evidence of inflammation driving secondary brain injury: a systematic review.* Journal of Trauma & Acute Care Surgery, 2015.

48.Hsiao, K.Y., H.S. Sun, and S.J. Tsai, *Circular RNA - New member of noncoding RNA with novel functions.* Exp Biol Med (Maywood), 2017. **242**(11): p. 1136-1141.

49.Iparraguirre, L., et al., *Circular RNA profiling reveals that circular RNAs from ANXA2 can be used as new biomarkers for multiple sclerosis.* Human molecular genetics, 2017. **26**(18): p. 3564-3572.

50.Jia, E., et al., *Transcriptomic profiling of circular RNA in different brain regions of*

Parkinson's disease in a mouse model. International Journal of Molecular Sciences, 2020. **21**(8): p. 3006.

51.Jiang, F., et al., *Circular RNAs as diagnostic biomarkers in gastric cancer: A meta-analysis review.* Pathology-Research and Practice, 2019. **215**(6): p. 152419.

52.Johnson, V.E., W. Stewart, and D.H. Smith, *Axonal pathology in traumatic brain injury.* Experimental Neurology, 2013. **246**(Sp. Iss. SI): p. 35-43.

53.Johnson, V.E., W. Stewart, and D.H. Smith, *Axonal pathology in traumatic brain injury.* Experimental neurology, 2013. **246**: p. 35-43.

54.Jungmann, A., et al., *Protocol for Efficient Generation and Characterization of Adeno-Associated Viral Vectors.* Hum Gene Ther Methods, 2017. **28**(5): p. 235-246.

55.Kristensen, L.S., et al., *The biogenesis, biology and characterization of circular RNAs.* Nature Reviews Genetics, 2019. **20**(11): p. 675-691.

56.Leo, P. and M. McCrea, *Frontiers in Neuroscience*

Epidemiology, in *Translational Research in Traumatic Brain Injury*, D. Laskowitz and G. Grant, Editors. 2016, CRC Press/Taylor and Francis Group

© 2016 by Taylor & Francis Group, LLC.: Boca Raton (FL).

57.Lewén, A., P. Matz, and P.H. Chan, *Free radical pathways in CNS injury.* J Neurotrauma, 2000. **17**(10): p. 871-90.

58.Li, T.-R., et al., *Circular RNA: a new star in neurological diseases.* International Journal of Neuroscience, 2017. **127**(8): p. 726-734.

59.Liu, S., et al., *The early growth response protein 1-miR-30a-5p-neurogenic differentiation factor 1 axis as a novel biomarker for schizophrenia diagnosis and treatment monitoring.* Transl Psychiatry, 2017. **7**(1): p. e998.

60.Liu, Y.W., S. Li, and S.S. Dai, *Neutrophils in traumatic brain injury (TBI): friend or foe?* J Neuroinflammation, 2018. **15**(1): p. 146.

61.Loane, D.J. and A. Kumar, *Microglia in the TBI brain: The good, the bad, and the dysregulated.* Exp Neurol, 2016. **275 Pt 3**(0 3): p. 316-327.

62.Lu, Y., L. Tan, and X. Wang, *Circular HDAC9/microRNA-138/Sirtuin-1 pathway mediates synaptic and amyloid precursor protein processing deficits in Alzheimer's disease.* Neuroscience bulletin, 2019. **35**(5): p. 877-888.

63.Lukiw, W., *Circular RNA (circRNA) in Alzheimer's disease (AD).* Frontiers in genetics, 2013. **4**: p. 307.

64.Lutton, E.M., et al., *Acute administration of catalase targeted to ICAM-1 attenuates*

neuropathology in experimental traumatic brain injury. Sci Rep, 2017. **7**(1): p. 3846.

65.Ma, N., et al., *Whole-transcriptome analysis of APP/PS1 mouse brain and identification of circRNA-miRNA-mRNA networks to investigate AD pathogenesis.* Molecular Therapy-Nucleic Acids, 2019. **18**: p. 1049-1062.

66.Marion, D.W., et al., *Effect of hyperventilation on extracellular concentrations of glutamate, lactate, pyruvate, and local cerebral blood flow in patients with severe traumatic brain injury.* Critical care medicine, 2002. **30**(12): p. 2619-2625.

67.Marklund, N., et al., *Evaluation of pharmacological treatment strategies in traumatic brain injury.* Current pharmaceutical design, 2006. **12**(13): p. 1645-1680.

68.Martin-Jiménez, C., et al., *Astrocytes Mediate Protective Actions of Estrogenic Compounds after Traumatic Brain Injury.* Neuroendocrinology, 2019. **108**(2): p. 142-160.

69.Mehta, S.L., R.J. Dempsey, and R. Vemuganti, *Role of circular RNAs in brain development and CNS diseases.* Prog Neurobiol, 2020. **186**: p. 101746.

70.Mellios, N., et al., *A set of differentially expressed miRNAs, including miR-30a-5p, act as post-transcriptional inhibitors of BDNF in prefrontal cortex.* Human molecular genetics, 2008. **17**(19): p. 3030-3042.

71.Morganti-Kossmann, M.C., et al., *Inflammatory response in acute traumatic brain injury: a double-edged sword.* Curr Opin Crit Care, 2002. **8**(2): p. 101-5.

72.Olde Heuvel, F., et al., *STAT6 mediates the effect of ethanol on neuroinflammatory response in TBI.* Brain, behavior, and immunity, 2019. **81**: p. 228-246.

73.Oliver, D.M.A. and P.H. Reddy, *Small molecules as therapeutic drugs for Alzheimer's disease.* Mol Cell Neurosci, 2019. **96**: p. 47-62.

74.Panda, A.C. and M. Gorospe, *Detection and Analysis of Circular RNAs by RT-PCR.* Bio-protocol, 2018. **8**(6): p. e2775.

75.Panda, A.C., et al., *Emerging roles and context of circular RNAs.* Wiley Interdiscip Rev RNA, 2017. **8**(2).

76.Paterno, R., K.A. Folweiler, and A.S. Cohen, *Pathophysiology and Treatment of Memory Dysfunction After Traumatic Brain Injury.* Curr Neurol Neurosci Rep, 2017. **17**(7): p. 52.

77.Pavlovic, D., et al., *Traumatic brain injury: neuropathological, neurocognitive and neurobehavioral sequelae.* Pituitary, 2019. **22**(3): p. 270-282.

78.Poon, H.F., et al., *Free radicals: key to brain aging and heme oxygenase as a cellular*

response to oxidative stress. J Gerontol A Biol Sci Med Sci, 2004. **59**(5): p. 478-93.

79.Povlishock, J.T. and H.A. Kontos, *The role of oxygen radicals in the pathobiology of traumatic brain injury.* Hum Cell, 1992. **5**(4): p. 345-53.

80.Qin, M., et al., *Hsa_circ_0001649: a circular RNA and potential novel biomarker for hepatocellular carcinoma.* Cancer Biomarkers, 2016. **16**(1): p. 161-169.

81.Ravnik-Glavač, M. and D. Glavač, *Circulating RNAs as Potential Biomarkers in Amyotrophic Lateral Sclerosis.* 2020. **21**(5).

82.Ravnik-Glavač, M. and D. Glavač, *Circulating RNAs as potential biomarkers in amyotrophic lateral sclerosis.* International journal of molecular sciences, 2020. **21**(5): p. 1714.

83.Roselli, F., et al., *Medusa's Head: The Complement System in Traumatic Brain and Spinal Cord Injury.* Journal of Neurotrauma, 2017: p. neu.2017.5168.

84.Roselli, F., et al., *Medusa's Head: The Complement System in Traumatic Brain and Spinal Cord Injury.* J Neurotrauma, 2018. **35**(2): p. 226-240.

85.Roux, A., et al., *Mass spectrometry imaging of rat brain lipid profile changes over time following traumatic brain injury.* Journal of neuroscience methods, 2016. **272**: p. 19-32.

86.Rungta, R.L., et al., *The cellular mechanisms of neuronal swelling underlying cytotoxic edema.* Cell, 2015. **161**(3): p. 610-621.

87.Ryan, B., G. Joilin, and J.M. Williams, *Plasticity-related microRNA and their potential contribution to the maintenance of long-term potentiation.* Frontiers in molecular neuroscience, 2015. **8**: p. 4.

88.Rybak-Wolf, A., et al., *Circular RNAs in the Mammalian Brain Are Highly Abundant, Conserved, and Dynamically Expressed.* Mol Cell, 2015. **58**(5): p. 870-85.

89.Santer, L., C. Bär, and T. Thum, *Circular RNAs: A Novel Class of Functional RNA Molecules with a Therapeutic Perspective.* Mol Ther, 2019. **27**(8): p. 1350-1363.

90.Sas, A., et al., *A review of neuroinflammatory mechanisms in ischemic stroke: background and therapeutic approaches.* Mech Neuroinflam, 2017. **119**.

91.Schmidt, O.I., et al., *Tumor necrosis factor-mediated inhibition of interleukin-18 in the brain: a clinical and experimental study in head-injured patients and in a murine model of closed head injury.* J Neuroinflammation, 2004. **1**(1): p. 13.

92.Shi, Z., et al., *The circular RNA ciRS-7 promotes APP and BACE1 degradation in an NF-κB-dependent manner.* The FEBS journal, 2017. **284**(7): p. 1096-1109.

93.Shlosberg, D., et al., *Blood–brain barrier breakdown as a therapeutic target in*

traumatic brain injury. Nature Reviews Neurology, 2010. **6**(7): p. 393-403.

94.Shohami, E., et al., *Endocannabinoids and traumatic brain injury.* British journal of pharmacology, 2011. **163**(7): p. 1402-1410.

95.Shohami, E., I. Ginis, and J.M. Hallenbeck, *Dual role of tumor necrosis factor alpha in brain injury.* Cytokine Growth Factor Rev, 1999. **10**(2): p. 119-30.

96.Simon, D.W., et al., *The far-reaching scope of neuroinflammation after traumatic brain injury.* Nat Rev Neurol, 2017. **13**(3): p. 171-191.

97.Spaethling, J., L. Le, and D.F. Meaney, *NMDA receptor mediated phosphorylation of GluR1 subunits contributes to the appearance of calcium-permeable AMPA receptors after mechanical stretch injury.* Neurobiology of disease, 2012. **46**(3): p. 646-654.

98.Sullivan, P.G., M.B. Thompson, and S.W. Scheff, *Cyclosporin A attenuates acute mitochondrial dysfunction following traumatic brain injury.* Experimental neurology, 1999. **160**(1): p. 226-234.

99.Sun, D.A., et al., *Traumatic brain injury causes a long-lasting calcium (Ca2+)-plateau of elevated intracellular Ca levels and altered Ca2+ homeostatic mechanisms in hippocampal neurons surviving brain injury.* European Journal of Neuroscience, 2010. **27**(7): p. 1659-1672.

100. Sun, D.A., et al., *Traumatic brain injury causes a long-lasting calcium (Ca2+)-plateau of elevated intracellular Ca levels and altered Ca2+ homeostatic mechanisms in hippocampal neurons surviving brain injury.* European Journal of Neuroscience, 2008. **27**(7): p. 1659-1672.

101. Szydlowska, K. and M. Tymianski, *Calcium, ischemia and excitotoxicity.* Cell Calcium, 2010. **47**(2): p. 122-9.

102. Tait, S.W. and D.R. Green, *Mitochondria and cell death: outer membrane permeabilization and beyond.* Nat Rev Mol Cell Biol, 2010. **11**(9): p. 621-32.

103. Tait, S.W.G. and D.R. Green, *Mitochondria and cell signalling.* Journal of cell science, 2012. **125**(Pt 4): p. 807-815.

104. Tuttolomondo, A., R. Pecoraro, and A. Pinto, *Studies of selective TNF inhibitors in the treatment of brain injury from stroke and trauma: a review of the evidence to date.* Drug design, development and therapy, 2014. **8**: p. 2221-2238.

105. Twohig, J.P., et al., *The role of tumor necrosis factor receptor superfamily members in mammalian brain development, function and homeostasis.* Rev Neurosci, 2011. **22**(5): p. 509-33

106. van Rossum, D., B.M. Verheijen, and R.J. Pasterkamp, *Circular RNAs: Novel Regulators of Neuronal Development.* Front Mol Neurosci, 2016. **9**: p. 74.

107. Wang, K.K., et al., *An update on diagnostic and prognostic biomarkers for traumatic brain injury.* Expert Rev Mol Diagn, 2018. **18**(2): p. 165-180.

108. Wang, P., et al., *Autophagy in ischemic stroke.* Progress in neurobiology, 2018. **163**: p. 98-117.

109. Weber, J.T., *Altered calcium signaling following traumatic brain injury.* Front Pharmacol, 2012. **3**: p. 60.

110. Woodcock, T. and C. Morganti-Kossmann, *The Role of Markers of Inflammation in Traumatic Brain Injury.* Frontiers in Neurology, 2013. **4**(18).

111. Woodcock, T. and M.C. Morganti-Kossmann, *The role of markers of inflammation in traumatic brain injury.* Front Neurol, 2013. **4**: p. 18.

112. Wu, F., et al., *Circular RNA TLK1 Aggravates Neuronal Injury and Neurological Deficits after Ischemic Stroke via miR-335-3p/TIPARP.* 2019. **39**(37): p. 7369-7393.

113. Wu, H., et al., *Simvastatin-mediated upregulation of VEGF and BDNF, activation of the PI3K/Akt pathway, and increase of neurogenesis are associated with therapeutic improvement after traumatic brain injury.* Journal of neurotrauma, 2008. **25**(2): p. 130-139.

114. Xia, X., et al., *A novel tumor suppressor protein encoded by circular AKT3 RNA inhibits glioblastoma tumorigenicity by competing with active phosphoinositide-dependent Kinase-1.* 2019. **18**(1): p. 131.

115. Xie, B.S., et al., *Circular RNA Expression Profiles Alter Significantly after Traumatic Brain Injury in Rats.* J Neurotrauma, 2018. **35**(14): p. 1659-1666.

116. Xiong, L.-L., et al., *Neural stem cell transplantation promotes functional recovery from traumatic brain injury via brain derived neurotrophic factor-mediated neuroplasticity.* Molecular neurobiology, 2018. **55**(3): p. 2696-2711.

117. Xiong, Y., et al., *Mitochondrial dysfunction and calcium perturbation induced by traumatic brain injury.* J Neurotrauma, 1997. **14**(1): p. 23-34.

118. Xu, K., et al., *Expression of aryl hydrocarbon receptor in rat brain lesions following traumatic brain injury.* Diagn Pathol, 2016. **11**(1): p. 72.

119. Xu, K., et al., *CircGRIA1 shows an age-related increase in male macaque brain and regulates synaptic plasticity and synaptogenesis.* 2020. **11**(1): p. 3594.

120. Xu, Y., et al., *miR-34a deficiency in APP/PS1 mice promotes cognitive function*

by increasing synaptic plasticity via AMPA and NMDA receptors. Neuroscience letters, 2018. **670**: p. 94-104.

121. Yi, L., et al., *Seawater Immersion Aggravates Early Mitochondrial Dysfunction and Increases Neuronal Apoptosis After Traumatic Brain Injury.* 2020. **40**(3): p. 447-457.

122. Yi, L., et al., *Seawater Immersion Aggravates Early Mitochondrial Dysfunction and Increases Neuronal Apoptosis After Traumatic Brain Injury.* Cellular and Molecular Neurobiology, 2020. **40**(3): p. 447-457.

123. You, X., et al., *Neural circular RNAs are derived from synaptic genes and regulated by development and plasticity.* Nat Neurosci, 2015. **18**(4): p. 603-610.

124. Zetterberg, H., D.H. Smith, and K. Blennow, *Biomarkers of mild traumatic brain injury in cerebrospinal fluid and blood.* Nature Reviews Neurology, 2013. **9**(4): p. 201-210.

125. Zhang, et al., *Role of mitochondrial calcium uniporter-mediated Ca2+ and iron accumulation in traumatic brain injury.* Journal of cellular and molecular medicine, 2019.

126. Zhang, J., et al., *Inhibition of Na+-K+-2Cl− cotransporter attenuates blood-brain-barrier disruption in a mouse model of traumatic brain injury.* Neurochemistry international, 2017. **111**: p. 23-31.

127. Zhang, L. and H. Wang, *Autophagy in traumatic brain injury: a new target for therapeutic intervention.* Frontiers in molecular neuroscience, 2018. **11**: p. 190.

128. Zhang, X., et al., *Bench-to-bedside review: Apoptosis/programmed cell death triggered by traumatic brain injury.* Crit Care, 2005. **9**(1): p. 66-75.

129. Zhang, Z., T. Yang, and J. Xiao, *Circular RNAs: promising biomarkers for human diseases.* EBioMedicine, 2018. **34**: p. 267-274.

130. Zhao, F., et al., *miR-30d-5p Plays an Important Role in Autophagy and Apoptosis in Developing Rat Brains After Hypoxic-Ischemic Injury.* Journal of Neuropathology & Experimental Neurology, 2017. **76**(8): p. 709.

131. Zhao, L. and Z. Wang, *MicroRNAs: Game changers in the regulation of α-synuclein in Parkinson's disease.* Parkinson's Disease, 2019. **2019**.

132. Zhong, S., et al., *CircPrimer: a software for annotating circRNAs and determining the specificity of circRNA primers.* BMC bioinformatics, 2018. **19**(1): p. 1-5.

133. Zuo, L., et al., *Circulating circular RNAs as biomarkers for the diagnosis and prediction of outcomes in acute ischemic stroke.* Stroke, 2020. **51**(1): p. 319-323.

134. Zuo, L., et al., *Circulating Circular RNAs as Biomarkers for the Diagnosis and Prediction of Outcomes in Acute Ischemic Stroke.* Stroke, 2020. **51**(1): p. 319-323.

7 Acknowledgements

Acknowledgements have been deleted for reasons of data protection.

8 Curriculum vitae

Curriculum vitae has been deleted for reasons of data protection.